Design, synthesis of novel triptolide-glucose conjugates targeting glucose Transporter-1 and their selective antitumor effect

Yan Liu, Jiaqing Huang, Min Wu, Bi Liu, Qiaofa Lin, Jingjing Wu, Yuhua Ouyang, Xin Guo, Ruyi Huang, Yongmin Zhang, et al.

Design, Synthesis of Novel Triptolide-Glucose Conjugates Targeting Glucose Transporter-1 and Their Selective Antitumor Effect

Yan Liu [a, b], Jiaqing Huang [a], Min Wu [a], Bi Liu [a], Qiaofa Lin [a], Jingjing Wu [a], Yuhua Ouyang [a], Xin Guo [a], Ruyi Huang [a], Yongmin Zhang [b, **] and Jianhua Xu [a, *]

[a] Department of Pharmacology, School of Pharmacy, Fuijan Provincial Key Laboratory of Natural Medicine Pharmacology, Fujian Medical University, Fuzhou 350122, China

[b] Sorbonne Université, CNRS, Institut Parisien de Chimie Moléculaire (IPCM), UMR 8232, 4 place Jussieu, 75005 Paris, France

KEYWORDS: triptolide • glucose transporter • triptolide-glucose conjugate • antitumor

ABSTRACT

Six positional isomers of triptolide–glucose conjugates (TG1α, TG1β, TG2, TG3, TG4 and TG6) were designed and synthesized. These conjugates exhibited better water solubility, and had selective cytotoxicity between the tumor cells with high expression of glucose transport-1 (Glut-1) and non-tumor cells with low expression of Glut-1, in which TG2 formed by triptolide (TPL) and D-glucose C2-OH had the strongest cytotoxicity to tumor cells and lowest toxicity in non-tumor cells, therefore the highest relative therapeutic index, which was 5.7 times that of triptolide and consequent the most powerful selective antitumor activity *in vitro*. The cytotoxicity of TG2 was highly correlated with Glut-1 function. As a prodrug of triptolide, TG2 could promote RNA Pol II degradation and induce apoptosis as TPL does. TG2 had a stronger dose-dependent antitumor effect *in vivo* than TPL and no adverse reaction occurred when its tumor inhibition was higher than 90%, which was associated with its selective distribution in tumor tissues. TG2 could be used as a promising drug candidate for the treatment of solid tumors with high expression of Glut-1, which is worthy of further study.

1. Introduction

Triptolide (TPL) is a triepoxide diterpene compound isolated from *Tripterygium wilfordii* which is mainly distributed in southern China, Japan and South Korea [1]. It has multiple pharmacological activities, such as antitumor, anti-inflammatory, anti-rheumatoid, anti-Alzheimer's disease, and immunosuppressive [2-5]. TPL has shown encouraging antitumor activity against various tumors *in vitro* and *in vivo* [6-8]. In the past decades, the development of TPL and its analogues as immunosuppressive drugs and antitumor drugs has been extensively studied [9-13].

There is a crucial need to address the safety problems caused by its narrow therapeutic window, poor water solubility, low selectivity and severe multiple organ toxicity (especially gastrointestinal, urogenital and bone marrow toxicity) [14-18]. Therefore, the major strategy to improve the application of triptolide was to selectively deliver it to tumor cells.

There are evidences that the reprogramming of energy metabolism performs a pivotal role in human tumor [19]. Even in sufficient oxygen, tumor cell still tends to produce ATP via glycolysis and convert glucose into intermediate metabolites needed for cell proliferation. Therefore, cancer cells need more molecules of glucose in comparison with normal cells [20]. It is well acknowledged that tumor cells are highly dependent on glucose for metabolism, and excessive expression of glucose transporters (Gluts) [21-23]. Among 14 Gluts reported so far, Glut-1 is likely one of the most extensively studied, whose overexpression has been identified in various tumors and correlates well

* Corresponding author. Department of Pharmacology, School of Pharmacy, Fuijan Provincial Key Laboratory of Natural Medicine Pharmacology, Fujian Medical University, Fuzhou 350122, China

** Corresponding author. E-mail addresses: xjh@fjmu.edu.cn (J. Xu), yongmin.zhang@upmc.fr ((Y. Zhang).

with poor prognosis [24]. Therefore, in virtue of the high expression of Glut-1 in tumor cells, glucose-bound cytotoxic drugs can be selectively transported to tumor cells by Glut-1, which is an effective strategy to improve the selectivity of cytotoxic drugs [25-26]. Researchers have found that antineoplastic drug glycosylation could improve its pharmacokinetic parameters, reduce side effects and prolong drug half-life in comparison with the parent compounds [27].

He et al. used succinic anhydride as the linker to conjugate triptolide C14-OH with D-glucose C1-OH through an ester bond to obtain the triptolide glucose conjugate Glutriptolide 2 which was more water-soluble and displayed better selectivity to tumor cells than triptolide, and proved to have sustained antitumor activity *in vivo* [28]. The other Glutriptolide was attained by changing the linker between D-glucose C1-OH and triptolide C14-OH, which still showed sustained antitumor activity [29]. However, the currently synthesized triptolide glucose conjugates were all formed by D-glucose C1-OH and triptolide [28,29]. Whether the conjugates constituted by D-glucose different positions hydroxyl groups and TPL have an influence on its antitumor efficacy and selectivity is the core issue that has not been reported so far.

Malay Patra et al. investigated the effects of different D-glucose substitution positions on the biological activity of platinum-glucose conjugates and revealed that the D-glucose substitution affected the vital features of the glucose conjugates for cell uptake, cytotoxicity profile, and Glut-1 specificity [30]. We used the crystal structure of Human Glut-1 (PDB ID: 5EQH) [31] to predict the interaction between D-glucose and Glut-1. The molecular docking results showed that the C3, C4, and C6 hydroxyl groups of D-glucose could form hydrogen bonding interactions with Glut-1 amino acid residues (Fig. S8), while the C1 and C2 hydroxyl groups of D-glucose could not form hydrogen bonds with Glut-1. Based on this, we assumed that the conjugates formed by modifications at the C1 or C2 positions of D-glucose would not interfere with their specific binding with Glut-1 and be transported into cells.

Accordingly, we structurally modify hydroxyl groups at C1, C2, C3, C4, and C6 of D-glucose to connect them with triptolide C14-OH through esterification using succinic acid as a linker to synthesize 6 triptolide-glucose conjugates (TG1α, TG1β, TG2, TG3, TG4 and TG6), among them except TG1α, TG1β having been reported by He [28]. It was found that TG2, synthesized by conjugated with triptolide and D-glucose C2-OH, had the strongest cytotoxicity to tumor cells and the lowest toxicity to non-tumor cells, therefore it had the highest relative therapeutic index (RTI) which was 5.7 of TPL. The RTI of TG2 was 2.5 times that of TG1β, of which TG1β was the most potent compound Glutriptolide 2 [28], hence TG2 had the strongest selective antitumor activity which was highly dependent on the functional level of Glut-1, suggested that C2-OH of D-glucose could be an ideal group for triptolide conjugation with D-glucose.

2. Results and discussion

2.1. Chemistry

Here, we attached triptolide C14-OH to different D-glucose substitution positions via a four-carbon ester bond of succinic anhydride to design and synthesize triptolide-glucose conjugates (TGs) (Fig. 1). The D-glucose exposing a free C1-OH residue was prepared according to the reported method [32]. Succinic anhydride was reacted with **1** in the mixture of DCM-DIPEA (10:1) at RT to obtain **2** with carboxyl linker. The esterification of triptolide with **2** was carried out in DCM, in which DMAP was the catalyst and EDCI was the dehydrating agent. All the benzyl groups in **3** were removed by H_2/Pd/C to afford **TG1** with a yield of 89% (Scheme 1).

The synthesis of **TG2-TG6** was initiated from D-glucose, which was treated with sodium acetate and acetic anhydride in reflux to obtain **15** with all hydroxyl groups protected by acetyl groups. The yield of synthetic intermediate **16** from **15** in one step using BnOH and $BF_3{\cdot}OEt_2$ was only 20%. Therefore, an alternative was performed, **15** was suffered 33% HBr to selectively transform anomeric acetyl group to bromine. The bromide was treated with BnOH in the presence of Ag_2CO_3 and I_2 to give the **16** in 82.8% yield at RT in the dark for 20 h. The C4 and C6 hydroxyl groups were selectively protected with benzylidene groups to attain **18**. Then **18** was treated with dibutyltin oxide, using TBAB and K_2CO_3 to selectively protect C2-OH or C3-OH with a benzyl group (Scheme S1). Since **4** (two compounds) eluted concurrently during the chromatographic purification process, the two compounds could not be separated and purified. What's more, only one compound could be observed by ^{1}H NMR, so we used this mixture in the next steps. **5** was directly conjugated with triptolide using EDCI/DMAP in DCM to give **6** with a yield of 62%. **6-2** and **6-3** can be separated and purified by preparative chromatography plate. The HMBC spectrum of **6-2** or **6-3** was shown in Fig. S1 and S2. Hydrogenolysis of **6-2** or **6-3** using Pd/C in MeOH:THF (1:1) generated **TG2**

or **TG3** with yields of 93% and 95%, respectively (Scheme 2). **19** was reduced by $NaBH_3CN$ and CH_3SiCl in dry DCM with 4Å MS to selectively achieve the C4 free hydroxyl group of **7**. Finally, **TG4** was prepared following a process similar to that described for the **TG1** (Scheme 3). The free hydroxyl group of C6 was obtained by reaction of compound **11** with 0.25 N MeONa at RT for 5 h to give **12**. Finally, **TG6** was prepared according to a procedure similar to **TG1** (Scheme 4). For the synthesis process of all compounds and the characterization of NMR (^1H, ^{13}C) spectra and HRMS of compounds, please refer to the supplementary information. The tests of oil-water partition coefficient (log *P*) found that the synthesized triptolide glucose conjugates (TGs) were more hydrophilic than their parent compound (Table 1).

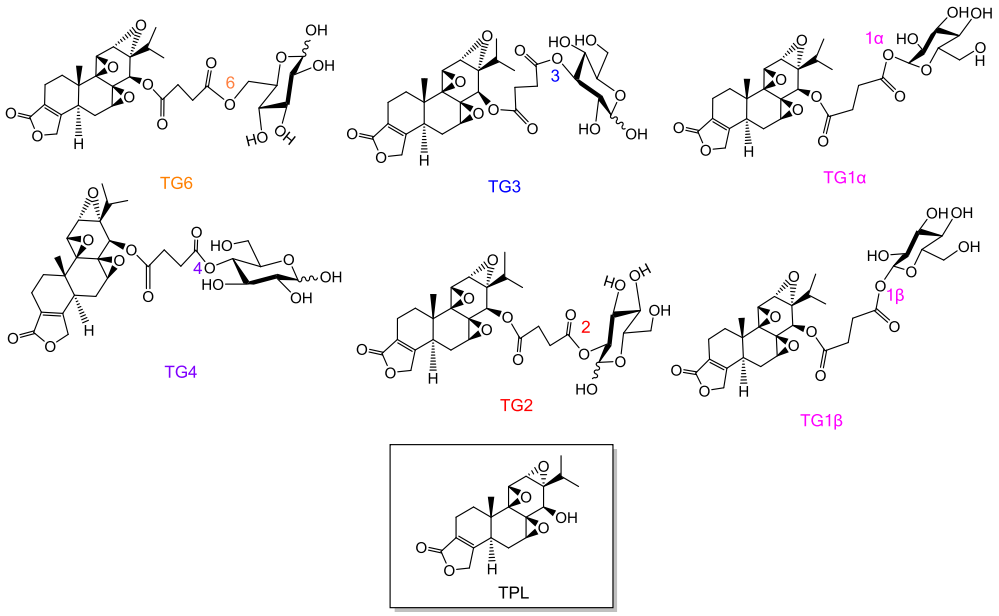

Fig. 1. Structures of C1-C6-substituted positional isomers (1-6) of triptolide-glucose conjugations and parent compound TPL.

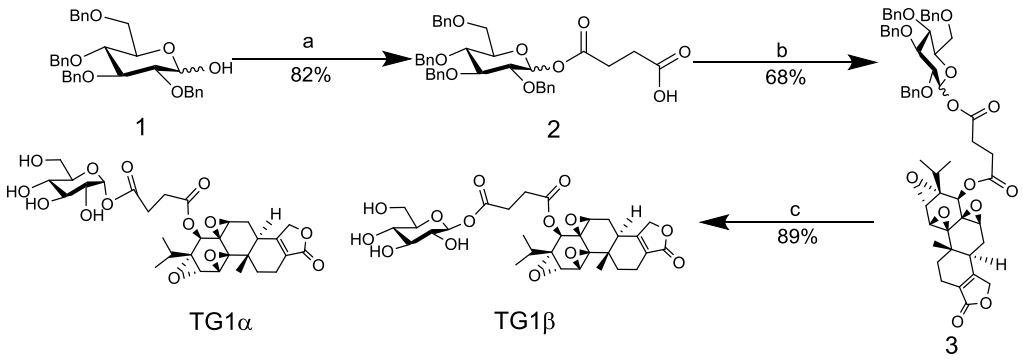

Scheme 1. Synthesis of compounds TG1. Reagents and conditions: (a) succinate anhydride, DCM, DIPEA, 82%; (b) triptolide, EDCI, DMAP, DCM, RT, 20 h, 68%; (c) H_2, Pd/C, MeOH, THF, RT, 3 h, 89%.

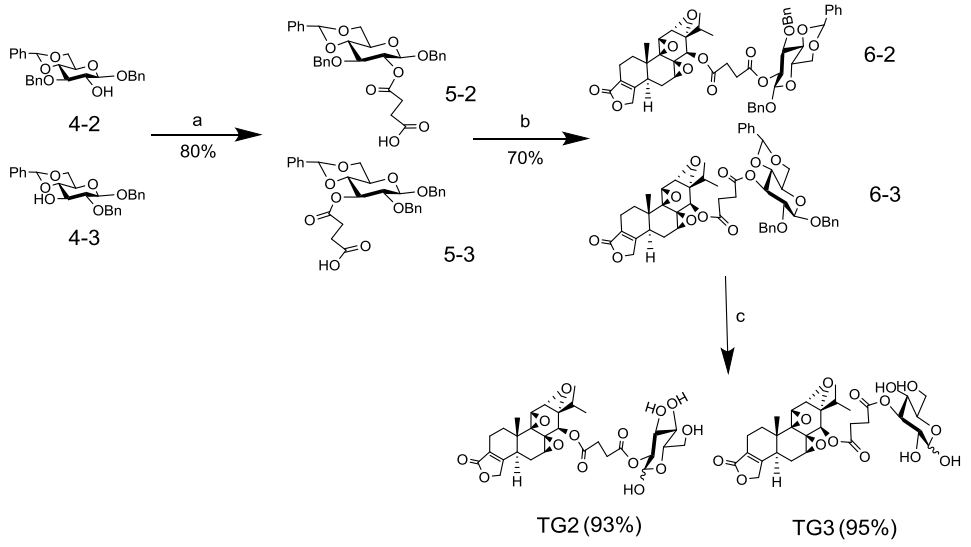

Scheme 2. Synthesis of compounds TG2 and TG3. Reagents and conditions: (a) succinic anhydride, DCM, DIPEA, 80%; (b) triptolide, EDCI, DMAP, DCM, rt, 20 h, 70%; (c) H_2, Pd/C, MeOH, THF, rt, 3 h, 93% (TG2) or 95% (TG3).

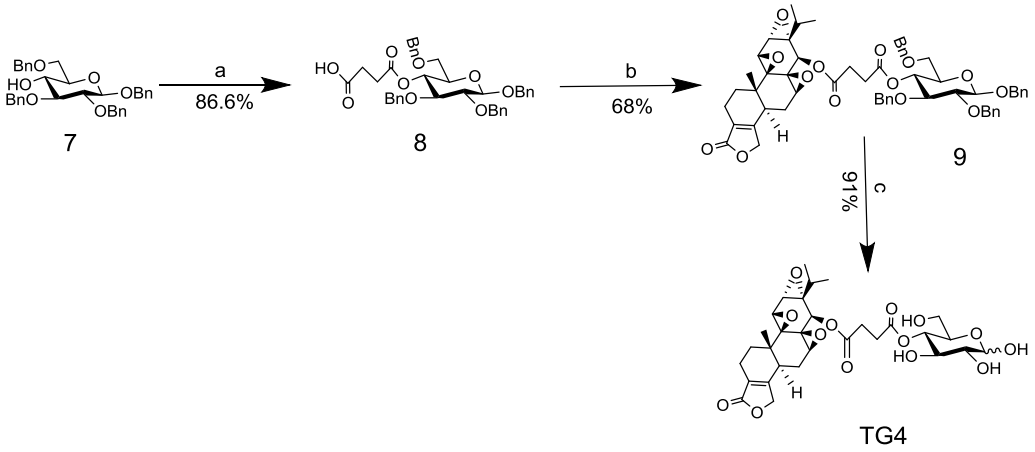

Scheme 3. Synthesis of compounds TG4. Reagents and conditions: (a) succinic anhydride, DCM, DIPEA, 86.6%; (b) triptolide, EDCI, DMAP, DCM, rt, 20 h, 68%; (c) H_2, Pd/C, MeOH, THF, rt, 3 h, 92%.

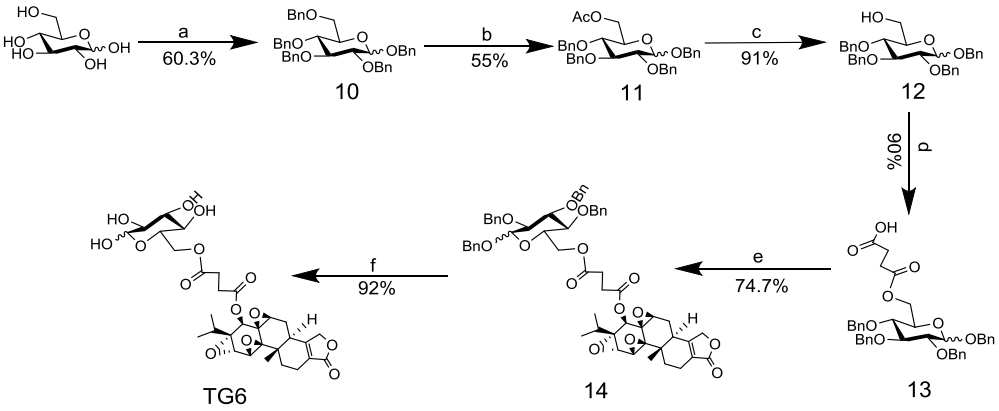

Scheme 4. Synthesis of compounds TG6. Reagents and conditions: (a) NaH, BnBr, DMF, 60.3%; (b) $ZnCl_2$, HOAc-Ac_2O, 55%; (c) NaOMe, MeOH, 91%; (d) succinic anhydride, DCM, DIPEA, 90%; (e) triptolide, EDCI, DMAP, DCM, rt, 20 h, 74.7%; (f) H_2, Pd/C, MeOH, THF, rt, 3 h, 89%.

Table 1

The oil-water partition coefficient values (log *P*) of triptolide and TGs.

Compound	log *P* (pH 7.4)
triptolide	-0.021±0.03
TG1β	-0.558±0.02
TG1α	-0.474±0.05
TG2	-0.347±0.04
TG3	-0.772±0.10
TG4	-0.331±0.05
TG6	-0.560±0.07

2.2. Selective antitumor activity of TGs

We tested the selective antitumor activity of TGs using MTT assay on between tumor cell lines (SW620, HCT116, HT29, MDA-MB-231, NCI-H460, NCI-H1975) with high expression of Glut-1 (Fig. S3) and non-tumor cell lines (HUVEC, LO2, HaCaT) with low expression of that (Fig. S3). With IC_{50} value for measuring cytotoxicity, the order of cytotoxicity potency of TGs on the tumor cell lines was as follows: TG2>TG3>TG1β>TG6>TG1α>TG4 (Table 2). Among them, TG2 with the lowest average IC_{50} on tumor cell lines had the strongest antitumor activity. Meanwhile the order of cytotoxicity potency of TGs on normal cell lines was as follows: TG6>TG4>TG3>TG1β>TG1α>TG2, suggesting TG2 has the lowest toxicity to non-tumor cells (Table 2). Taking advantage of the relative therapeutic index (RTI, $IC_{50\ \text{non-tumor mean}}/IC_{50\ \text{tumor mean}}$) to measure selective cytotoxicity to tumor cells, the order of TGs selective cytotoxicity on the tumor cell lines was as follows: TG2>TG3>TG1β>TG1α>TG6>TG4>TPL (Table 2). The outcomes indicated that TG2 formed by conjugating D-glucose C2-OH with TPL had the highest selectivity to tumor cells, followed by TG3, TG1β and TG1α. The RTI of TG2, TG3, TG1β or TG1α was 5.7, 2.5, 2.3 and 1.9 times that of TPL, respectively. The results in Table 2 indicated that the RTI of TG2 was 2.5 times that of TG1β namely Glutriptolide 2 reported by He [28]. Furthermore the potency of TG2 on tumor cell lines (Mean IC_{50} = 1.79 μM) is about 1.64 times that of TG1β (Mean IC_{50} = 2.94 μM). Our results demonstrated that TG2 not only had the strongest anti-tumor activity but also the highest selectivity to tumor cells, suggesting the D-glucose C2-OH is an ideal site for conjugating with TPL, and the resulting TG2 may be most easily transported into tumor cells through glucose transporters.

Table 2

IC_{50} values of triptolide and TGs against tumor or non-tumor cell lines and their relative therapeutic index.

Cell line	Compound (Mean ± SD, μM)						
	TPL	TG1β	TG1α	TG2	TG3	TG4	TG6
SW620	0.163±0.018	5.512±1.511	3.855±1.078	1.725±0.649	2.547±0.316	10.974±0.567	5.203±0.065
MDA-MB-231	0.051±0.024	2.280±0.202	4.419±0.331	1.973±0.533	2.427±0.747	5.607±1.243	6.618±1.028
HCT116	0.046±0.021	2.354±0.585	1.904±0.265	1.952±0.440	2.711±0.556	4.467±0.677	2.279±0.492
HT29	0.047±0.001	2.889±0.109	5.374±0.169	2.190±0.513	5.180±0.648	4.078±1.127	4.283±1.246
NCI-H460	0.014±0.001	2.722±1.108	4.081±1.194	0.870±0.125	1.632±0.018	3.061±0.129	1.069±0.130
NCI-H1975	0.002±0.012	1.859±0.661	3.421±0.239	2.038±0.228	2.213±0.075	2.508±0.344	1.140±0.256
Mean ± SD	0.054±0.057	2.936±1.312	3.842±1.115	1.791±0.476	2.785±1.231	5.116±3.069	3.432±2.228
HUVEC	0.044±0.013	8.137±1.503	5.678±0.284	8.554±0.431	4.930±1.024	2.358±0.262	2.020±0.155
LO2	0.016±0.001	1.378±0.034	2.146±0.808	1.317±0.388	1.375±0.140	1.798±0.088	1.415±0.131
HaCaT	0.027±0.009	1.633±0.391	4.295±0.118	6.544±1.796	4.828±2.129	4.753±0.338	3.896±1.034
Mean ± SD	0.029±0.014	3.716±3.831	4.040±1.780	5.472±3.736	3.711±2.024	2.970±1.570	2.444±1.294
RTI	0.539	1.266	1.051	3.055	1.332	0.580	0.712

RTI: Relative Therapeutic Index = $IC_{50\ non\ tumor\ mean}/IC_{50\ tumor\ mean}$

2.3. TGs cytotoxicity is associated with Glut-1 function or expression level

Given that TGs were glucose conjugates of triptolide, their selective cytotoxicity on tumor cells may be due to the high expression of Glut-1 in tumor cells. In order to observe the effect of Glut-1 function or expression level on TGs anti-tumor activity in the same genetic background, we treated NCI-H460 cells with TGs combing with Glut-1 inhibitors or Glut-1 siRNA. The Glut-1 expression of Glut-1 silenced NCI-H460 cells was much lower than that of vector-transfected NCI-H460 cells (Fig. S4).

It was shown that in the presence of Glut-1 inhibitors the dose-effect curve of TGs on cell viability moved right accordingly the IC_{50} values of TGs to NCI-H460 cells were increased in varying degrees (Fig. 2). Similar results were found in Glut-1 silenced NCI-H460 cells, namely the rising IC_{50} of TGs was found in Glut-1 knockdown NCI-H460 cells (Fig. 3). These data demonstrated that the cytotoxicity of TGs was positively associated with Glut-1 function or expression level, but that of TPL was not. Among all TGs, the increase of IC_{50} for TG2 was the most significant whether in the presence of Glut-1 inhibitors or Glut-1 knockdowns (Fig. 2H, 3H), suggested the cytotoxicity of TG2 was most affected by Glut-1, which was the antitumor activity of TG2 may be more relying on Glut-1. Since TG2 had the strongest selective antitumor activity, therefore we further studied the antineoplastic properties of TG2.

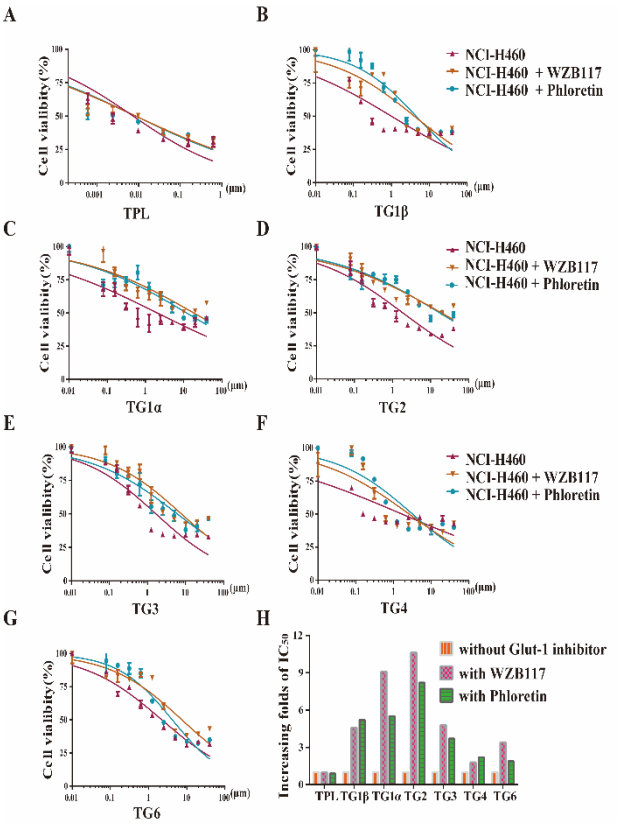

Fig. 2. The cytotoxicity of TGs on NCI-H460 cells in the presence of Glut-1 inhibitor. (A-G) TGs cytotoxicity was declined in combination with TGs with Glut-1 inhibitors 10 μM WZB117 or 100 μM Phloretin. (H) The increasing folds of IC_{50} for TGs in the presence of Glut-1 inhibitors 10 μM WZB117 or 100 μM Phloretin. Cell viability was measured by MTT assay. Data represent the mean ± SD of at least three or more replicates.

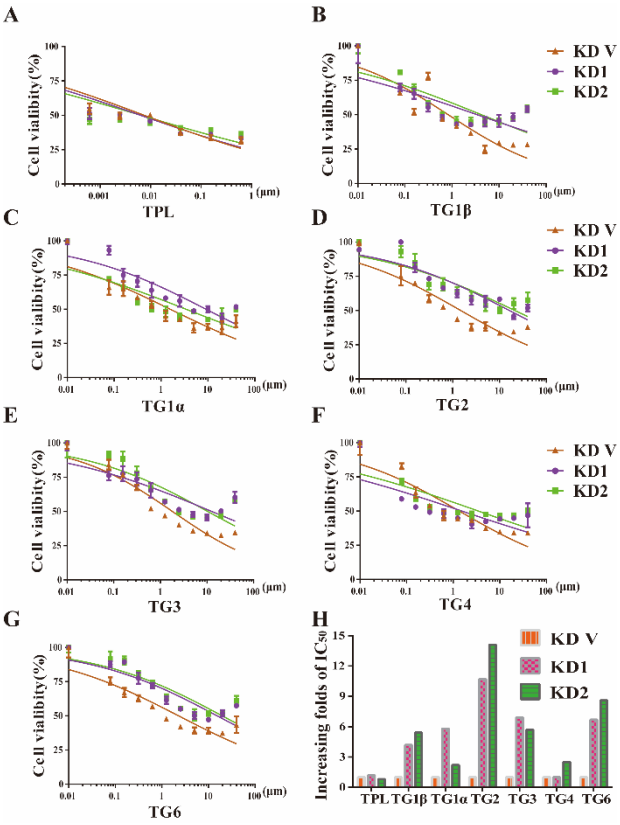

Fig. 3. The cytotoxicity of TGs on Glut-1 silenced NCI-H460 cells. (A-G) Glut-1 knockdown declined TGs cytotoxicity in NCI-H460 cells, Glut-1 knockdown with KD1 or KD2, using the vector (KD V) for control. (H) The increasing folds of IC_{50} for TGs when Glut-1 knockdown. Cell viability was measured by MTT assay. Data represent the mean ± SD of at least three or more replicates.

2.4. Selective effect of TG2 is highly dependent on Glut-1 of tumor cells

In order to compare the cytotoxic effect of TG2 on tumor cells and non-tumor cells with different Glut-1 expression levels, we utilized both tumor and non-tumor cell lines in different Glut-1 levels produced by knockdown or overexpression to assess the cytotoxicity of TG2 or TPL. It was found that the dose-effect curve of TG2 moved right with Glut-1 knockdown (Fig. 4B) and moved left with Glut-1 overexpression (Fig. 4C, D), which suggested that the cytotoxicity of TG2 to cells increased with the level of Glut-1. However, the degree of this change for tumor cells (NCI-H1975) was greater than that for non-tumor cells (HUVEC) (Fig. 4E), which implied that TG2 may be safety in normal cells even though their Glut-1 expression may be a bit high in a few normal cells in some cases, however its cytotoxicity may not be enhanced proportionately.

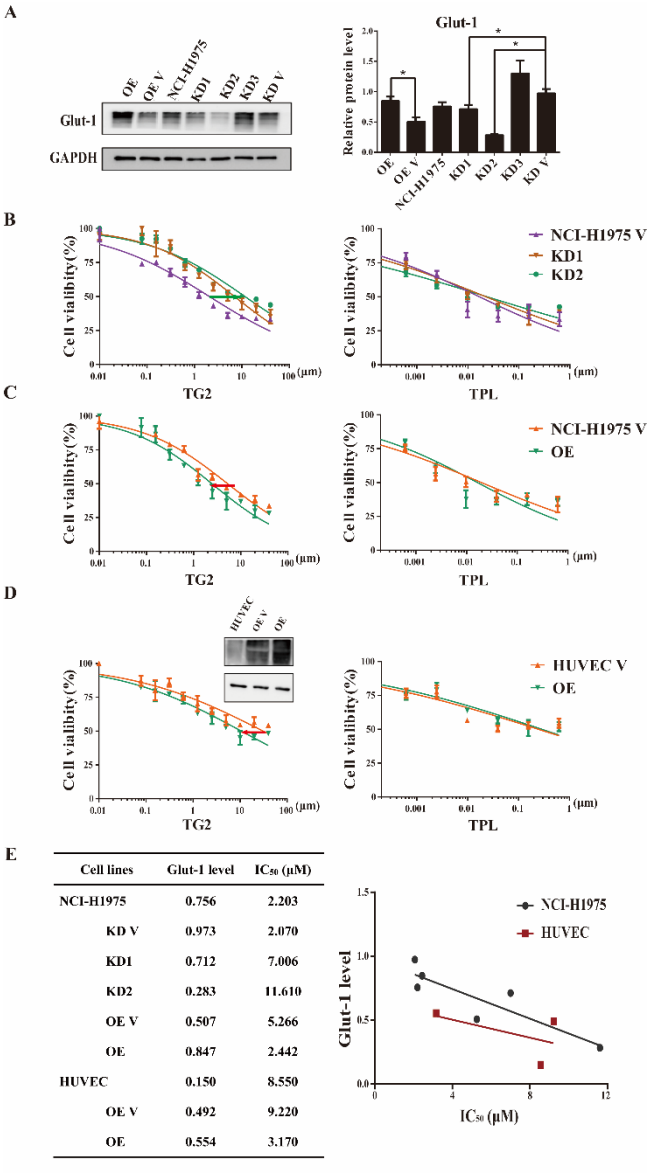

Cell lines	Glut-1 level	IC_{50} (μM)
NCI-H1975	0.756	2.203
KD V	0.973	2.070
KD1	0.712	7.006
KD2	0.283	11.610
OE V	0.507	5.266
OE	0.847	2.442
HUVEC	0.150	8.550
OE V	0.492	9.220
OE	0.554	3.170

Fig. 4. The cytotoxicity of TG2 was dependent on Glut-1 expression level. (A) Expression levels of Glut-1 in silenced or overexpressed in NCI- H1975 cells determined by Western blotting. (B) Glut-1 knockdown declined TG2 cytotoxicity but not TPL in NCI-H1975 cells. Cell viability was measured by MTT assay. Data represent the mean ± SD of at least three or more replicates. (C) Glut-1 overexpression enhanced TG2 cytotoxicity but not TPL in NCI-H1975 cells. Cell viability was measured by MTT assay. Data represent the mean ± SD of at least three or more replicates. (D) Glut-1 high overexpression raised TG2 cytotoxicity lightly in HUVEC cells. Expression levels of Glut-1 overexpressed in HUVEC cells determined by Western blotting. Cell viability was measured by MTT assay. Data represent the mean ± SD of at least three or more replicates. (E) Glut-1 level was negatively correlated with the IC_{50} value of TG2 in NCI-H1975 and HUVEC cells with different levels of Glut-1 expression. Whole cell lysates were resolved by SDS-PAGE and analyzed by immunoblotting against either Glut-1 and GAPDH (loading control). Cell viability was measured by MTT assay. The data represents the mean ± SD of at least three replicate samples. *: $p<0.05$, compared with the overexpressed vector (OE V) or the knockdown vector (KD V).

2.5. TG2 induces RNA pol II degradation and apoptosis in tumor cells

Triptolide-glucose conjugates were able to be hydrolyzed via esterase in cells to release triptolide and intermediates (triptolide succinate) [28]. The main target of TPL for its antitumor activity was RNA Pol II which was degragated by TPL [33-37]. As an inhibitor of RNA polymerase I and II-dependent transcription, TPL mainly resulted in the down-regulation of short-lived mRNA, which associated with its inhibition of proliferation and induction of apoptosis in cancer cells [38]. As a prodrug of TPL, TG2 may induce RNA pol II degradation as TPL does. We found that both TG2 and TPL promoted RNA pol II degradation after NCI-H640 cells exposed the drugs for 48 h, however TG2 had a weaker influence on RNA pol II than TPL (Fig. 5).

TPL induces tumor cell apoptosis by down-regulating a large number of proteins which play a key role in anti-apoptosis (Bcl-2, Mcl-1, Bcl-xL, XIAP, C-IAP1, C-IAP2) [39-41]. The dissipation of mitochondrial membrane potential (MMP) occurred in the initial stage of cell apoptosis. Moreover, excessive ROS production affects mitochondrial permeability and cytochrome C release and results in apoptosis [42]. We measured MMP using the TMRE probe. Both TG2 and TPL could reduce the relative fluorescence intensity of TMRE and attenuate the accumulation of TMRE (Fig. S5), suggesting MMP dissipation. An increased intensity of DCF fluorescence occurred in NCI-H460 cells following TG2 or TPL treatment, suggesting that ROS accumulation was enhanced (Fig. 6A, B), which could result in an apoptotic induction notably in a dose-dependent manner (Fig. 6C, D). The outcomes exhibited that TG2 same as TPL could induce the dissipation of MMP, promote the generation of ROS, subsequently result in apoptosis.

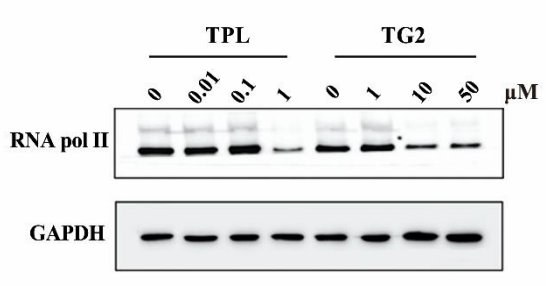

Fig. 5. TPL or TG2 promoted RNA pol II degradation. The protein level of RNA Pol II of NCI-H460 cells treated with TG2 or triptolide for 48 h analyzing with Western blotting. Whole cell lysates were resolved by SDS-PAGE and analyzed by Western blotting against either RNA Pol II and GAPDH (loading control).

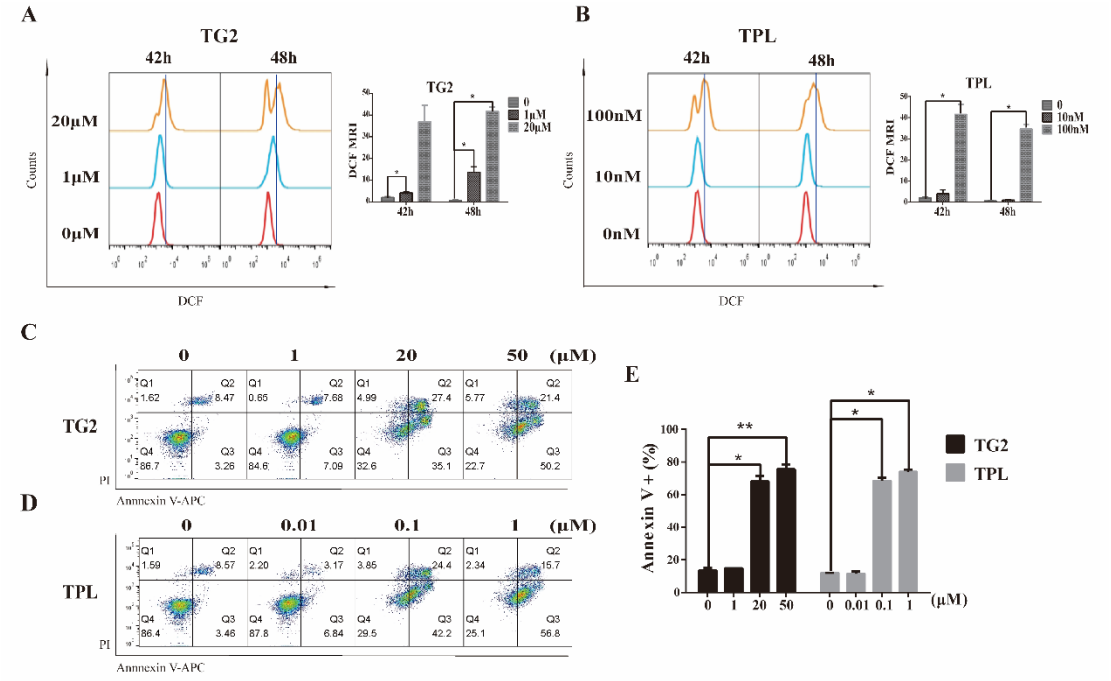

Fig. 6. TG2 induced ROS accumulation and cell apoptosis. (A) Effect of TG2 on ROS in NCI-H460 cells exposing for 42 h or 48 h. The ROS was measured by DCFH-DA. MFI = Mean Fluorescence Intensity. DCF fluorescence was calculated compared with the control and the results were expressed as the percentage of fluorescence which obtained from the histogram statistics. (B) Effect of TPL on ROS in NCI-H460 cells exposing for 42 h or 48 h. DCF fluorescence was calculated compared with the control and the results were expressed as the percentage of fluorescence which obtained from the histogram statistics. (C) Effect of TG2 on apoptosis of NCI-H460 cells exposing for 48 h. (D) Effect of triptolide on apoptosis of NCI-H460 cells exposing for 48 h. (E) The histogram of apoptosis rate of NCI-H460 cells treated with TG2 or TPL at 48 h. Data represent the mean ± SD of at least three or more replicates. *: $p<0.05$, **: $p<0.01$, compared with the control.

2.6. TG2 has high antitumor effect *in vivo*

Lung cancer is the most common malignant tumor in human beings. Non-small cell lung cancer (NSCLC) accounts for about 85% of all lung cancers [43]. The IC_{50} of TG2 on NSCLC cell line NCI-H1975 was 2.038 μM (Table 2), and NCI-H1975 cells carried EGFR T790M mutation were resistant to the first generation of EGFR-TKI (epidermal growth factor-receptor-tyrosine kinase inhibitor) [44,45]. Thereby, we established a nude mouse xenograft model of NCI-H1975 cells to evaluate TG2 antitumor effect *in vivo*. It was found that NCI-H1975 bearing mice treated with Paclitaxel (PTX) (15 mg/kg, ip, q3d×6), TPL (0.2 mg/kg, ip, qd, d1-d5/week×2), TG2 (1 mg/kg, ip, qd, d1-d5/week×2) and TG2 (2 mg/kg, ip, qd, d1-d5/week×2) resulted in tumor weight inhibition rates by 56.92%, 28.65%, 75.44% and 90.42%, respectively (Fig. 7D). The expression of RNA pol II in tumor tissue was detected by Western blotting, as showed in Fig. S6 that TG2, similar to its parent drug TPL, induced RNA pol II degradation in tumor tissue, which was consistent with its effect *in vitro*. The antitumor effect of TG2 (1 mg/kg and 2 mg/kg) was significantly stronger than that of PTX (15 mg/kg), a first-line chemotherapy drug for NSCLC and of its parent compound TPL (0.2 mg/kg) (Fig. 7B, C, D). During the experiment period, no adverse reactions such as remarkable weight loss (Fig. 7A) and diarrhea were found in each group of tumor-bearing mice. TG2 showed strong antineoplastic activity against NCI-H1975, proposed that it may have potential clinical value in the treatment of NSCLC with $EGFR^{L858R/T790M}$ mutation.

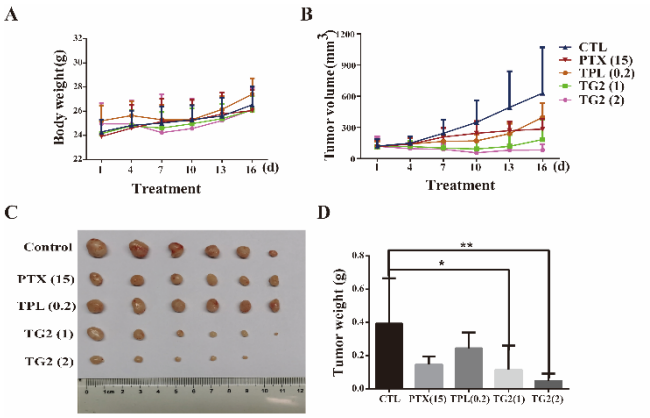

Fig. 7. Antitumor effects of TG2 on NCI-H1975 xenograft tumor models *in vivo*. (A) Body weight curves of the NCI-H1975 tumor-bearing mice in the different groups throughout the 2 week-treatment. (B) Tumor growth curves of the NCI-H1975 tumor-bearing mice in the different groups throughout the treatment. (C) Photographs of the tumors removed from the different groups of tumor-bearing mice after treatment. (D) The effects of TG2 on tumor weight in the different groups of the tumor-bearing mice after the 2 week-treatment. *: $p<0.05$, **: $p<0.01$, compared with the control.

2.7. The high efficient dose of TG2 has lower toxicity *in vivo* than TPL

It was reported that 0.2 mg/kg of TPL was an effective dose which could produce obvious antitumor activity *in vivo* [28]. In order to compare the toxicity of TG2 and TPL at their therapeutic dose, the heart, liver, lung and kidney of mice in each group as well as testis tissue that was most sensitive to TPL [46] were taken for section and H&E stain at the end of the experiment. The results showed that the morphological structures of heart, liver, lung and kidney in TG2 (1 mg/kg and 2 mg/kg) and TPL (0.2 mg/kg) groups had no significant difference compared with the control group (Fig. S7). However, for TPL sensitive testis tissue, irregular spermatogenic tubules, reduced cytoplasmic vacuoles and nuclei, decreased spermatogenic cells, and degeneration of intertubule connective tissue were observed in the TPL group (Fig. 8B). Similar changes were also observed in the TG2 (2 mg/kg) group, however, the pathologic morphological change degree of testis tissue in the TG2 (2 mg/kg) group was less severe than that in the TPL (0.2 mg/kg) group (Fig. 8D), while there was no significant change in testis morphological structure in the TG2 (1 mg/kg) group compared with the control group (Fig. 8A, C). According to above, it was suggested that the effect of TG2 (1 and 2 mg/kg), a high efficient dose, on testis tissue, which was most sensitive to TPL, was notably lower than that of triptolide (0.2 mg/kg), a slight efficient dose in xenograft model of NCI-H1975.

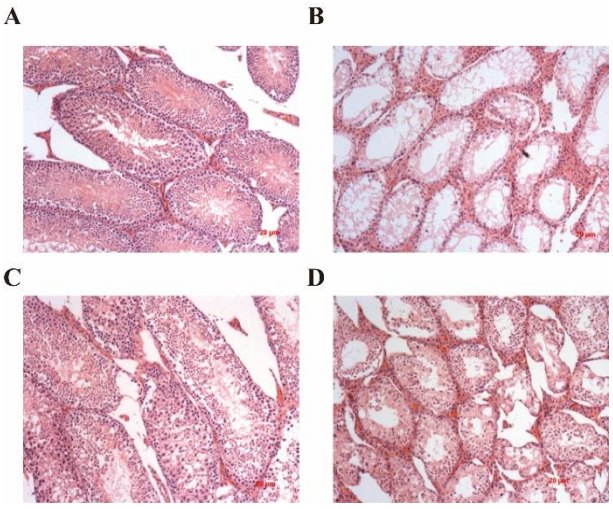

Fig. 8. Effect of TG2 and TPL on the morphological structure of testis (H&E stain, ×200). (A) Normal control (saline); (B) TPL (0.2 mg/kg); (C) TG2 (1 mg/kg); (D) TG2 (2 mg/kg).

2.8. TG2 is stable in serum and selectively distributed in tumor tissues *in vivo*

Since esterase in plasma is abundant, the ester bond of TG2 could be hydrolyzed by certain esterases and release TPL in plasma, which might cause adverse reaction. Hence we explored the stability of TG2 in serum and the distribution of TG2 in major organs and tumor tissue *in vivo*. When TG2 was incubated with mouse or human serum at different time points, the content of TPL released from TG2 to be detected *in vitro*. It was found that TG2 incubated with mouse serum for 8 h, it still existed in its original form, and there was no detectable TPL released. When incubation time extended to 72 h, 66% of TG2 was still present in its original form (Fig. 9A). It was suggested that TG2 was stable at least within 8 h in mice serum. The similar stability of TG2 was found in human serum (Fig. S9). After intravenous injection of TG2 (1 mg/kg) in nude mice, the pharmacokinetic parameters $AUC_{0\sim3h}$, $MRT_{0\sim3h}$ and $t_{1/2}$ were 83.62 μmol/L*h, 0.56 h and 0.32 h, respectively (Fig. 9B). It revealed that TG2 was almost disappeared in plasma 2 h (went through about 6 folds of $t_{1/2}$) after intravenous injection. Since the time of TG2 stabilization in serum (8 h) *in vitro* was considerably longer than that of its existence in plasma (2 h) *in vivo*. Therefore, TG2 exists only for a short time in mouse plasma and its resistance from esterase hydrolysis keeps for a relative long time, consequently with little possibility to release TPL in mouse plasma. That is, TG2 was stable in the blood of mice before entering tissues. In order to verify whether TG2 was preferentially distributed in tumor tissues, samples of hearts, livers, lungs, kidneys and tumor were collected from NCI-H1975 tumor-bearing mice after intravenous injection of TG2 or TPL, and the contents of TG2, TPL and TG2 metabolites in these samples was detected by LC-MS. The LC-MS analysis shows that TG2 was hydrolyzed to triptolide and intermediates (triptolide succinate) in tissues. We found that after administration in TG2 (2 mg/kg) group for 1 h (went through about 3 folds of $t_{1/2}$), the contents of TG2 and its metabolites in tumor tissues were 9.3, 18.8, 15.5 and 7.3 times of those in liver, kidney, lung and heart, respectively, suggesting that TG2 would selectively distribute in tumor tissues. However, there was no selective distribution of triptolide between tumor and organs tissues after administration (Fig. 9C). Fig. 9C showed that even now triptolide succinate was the main hydrolytic product of TG2 in tumor tissues, it could subsequently continue to be hydrolyzed by esterase and ultimately released triptolide to produce sustained antitumor effects.

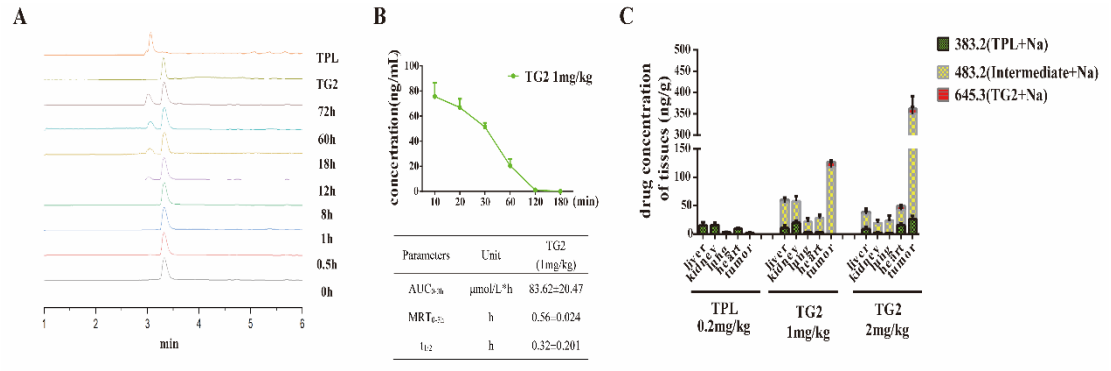

Fig. 9. TG2 is stable in serum and selectively distributed in tumor tissues *in vivo.* (A) The stability of TG2 incubated in mice serum at different times. (B) The concentration-time curve of TG2 in plasma following intravenous injection of TG2 (1 mg/kg). The concentration of TG2 (MW: 645.3) in plasma samples was detected by LC-MS. Data represent the mean ± SD, n=3. (C) The tissue distribution of TG2 or TPL *in vivo*. After intravenous injection TG2 or triptolide (0.2 mg/kg) for 1 h, heart, liver, lung, kidney, and tumor tissues from NCI-H1975 tumor-bearing mice were collected. The concentration of TG2 (MW: 645.3) and TG2 metabolites: triptolide succinate (MW: 483.3) and triptolide (MW: 383.2) in tissue samples of tumor or organs were detected by LC-MS. Data represent the mean ± SD, n=3.

3. Conclusions

Taken together, six triptolide-glucose conjugates have been designed and synthesized by using succinic anhydride as a linker between D-glucose C1, C2, C3, C4 and C6-OH and triptolide C14-OH. Among them, TG2 formed by triptolide and D-glucose C2-OH has the

strongest selective cytotoxicity to tumor cells. The cytotoxicity of TG2 increased with the high expression of Glut-1, and the effect was more obvious in tumor cells than in non-tumor cells, indicating the cytotoxicity of TG2 to normal cells was lower. As a prodrug of triptolide, TG2 has a similar target with triptolide, both of them can promote RNA Pol II degradation and induce apoptosis. TG2 is stable in serum and selectively distributed in tumor tissues, therefore has a powerful dose-dependent antitumor effect and low toxicity on NCI-H1975 xenografts models.

4. Experimental

4.1. General Procedures of Chemistry

All chemicals were acquired from commercial suppliers as reagent grade quality or better, and used without further purification. All reactions proceed under argon atmosphere and anhydrous conditions unless aqueous reactions. Solvents were used as received or dried over molecular sieves.

The reaction was monitored by thin-layer chromatography (TLC) on a pre-coated plate of silica gel 60 F254 (Merck) and detected by ultraviolet light and/or sulfuric acid carbonization. Evaporation of the solvent was performed under reduced pressure below 40 ℃ (water bath). Column chromatography was carried out on silica gel 60 (230-400 mesh, Merck).

^{1}H NMR and ^{13}C NMR spectra were measured on Bruker AVANCE DRX 400 spectrometers at 25 ℃. All the measurements were carried out using deuterated solvents. The chemical shifts were referenced relative to trace amounts of the solvent peak, 7.26 ppm (^{1}H) and 77.16 ppm (^{13}C) for $CDCl_3$, 3.31 ppm (^{1}H) and 49.00 ppm (^{13}C) for CD_3OD at 25 ℃, and are described in parts per million (ppm). Coupling constants (J) are indicated in Hertz (Hz), with multiplicity mentioned following the usual convention: s, singlet; d, doublet; t, triplet; q, quadruplet; dd, doublet of doublets; ddd, doublet of doublet of doublets; dt, doublet of triplets; dq, doublet of quartets; m, multiplet; brs, broad singlet. ESI mass spectra were recorded on an AgilentS3 Technologies 1100 series LC-MSD trap. High-resolution mass spectra (HRMS) were conducted with a Bruker micro TOF spectrometer in electrospray ionization (ESI) mode, using Tuning-Mix as reference.

Synthesis of Succinic Acid Mono-((3R,4S,5R,6R)-3,4,5-tris(benzyloxy)-6-((benzyloxy) methyl) tetrahydro-2H-pyran-2-yl) Ester (2). Compound **1** was synthesized as previously reported [32]. **1** (0.92 g, 1.704 mmol) dissolved in DCM–DIPEA (10:1, 6.6 mL) was treated with succinic anhydride (0.852 g, 8.52 mmol), stirred at RT for 20 h then eliminated the solvent. The residue was dissolved in EtOAc (30 mL), washed with brine, saturated $NaHCO_3$ (aq), dried over Na_2SO_4, and concentrated. The residue was purified through silica gel column chromatography (CH_2Cl_2/CH_3OH, 50:1) to give compound **2** as a colorless syrup (0.894 g, 82%). ^{1}H NMR (400 MHz, Chloroform-*d*) δ 7.41 – 7.18 (m, 20H), 5.65 (d, J = 8.0 Hz, 1H), 4.99 – 4.87 (m, 1H), 4.86 – 4.79 (m, 2H), 4.77 (s, 1H), 4.71 – 4.58 (m, 2H), 4.57 – 4.46 (m, 2H), 3.81 – 3.66 (m, 4H), 3.64 – 3.52 (m, 2H), 2.76 – 2.53 (m, 4H). ESI-MS *m/z* calcd for $C_{38}H_{40}O_9Na$ $[M+Na]^+$ 663.2570, found 663.2653.

Synthesis of (5bS,6aS,7aR,8aS,9aS,9bS,10aS,10bS)-8a-isopropyl-10b-methyl-3-oxo-1,2,3,5,5b,6, 6a,8,8a,9a,9b,10b-dode cahydrotris(oxireno) [2',3':4b,5;2'',3'': 6,7;2''', 3''':8a,9] phenanthro[1,2-c]furan-8-yl((3R,4S,5R,6R)-3,4,5-tris (benzyloxy)-6-((benzyloxy)methyl)tetr- ahydro-2H-pyran-2-yl) succinate (3). To a mixture of triptolide (36 mg, 0.1 mmol), **2** (76.8 mg, 0.12 mmol), EDCI (38.34 mg, 0.2 mmol), DMAP (3.66 mg, 0.03 mmol) dissolved in dry CH_2Cl_2 (3 mL) was stirred for 20 h at RT. The resulting mixture was dissolved in CH_2Cl_2 (5 mL), washed with water (5 mL), brine (5 mL) and saturated $NaHCO_3$ (aq) (5 mL), dried over Na_2SO_4, then evaporated to give a residue. The residue was purified by silica gel column chromatography (Cy-EtOAc, 3:1, twice) to give the compounds **3** as a white solid (66.8 mg, 68%). ^{1}H NMR (400 MHz, Chloroform-*d*) δ 7.47 – 7.21 (m, 18H), 7.15 (dd, J = 6.9, 2.8 Hz, 2H), 5.63 (d, J = 8.0 Hz, 1H), 5.09 (s, 1H), 4.90 (d, J = 10.9 Hz, 1H), 4.86 – 4.77 (m, 3H), 4.70 – 4.63 (m, 2H), 4.62 (s, 1H), 4.55 (d, J = 10.6 Hz, 1H), 4.52 – 4.46 (m, 1H), 3.80 – 3.69 (m, 4H), 3.65 – 3.54 (m, 2H), 3.50 (d, J = 3.1 Hz, 1H), 3.44 (d, J = 5.4 Hz, 1H), 2.86 – 2.56 (m, 5H), 2.32 (dd, J = 18.3, 4.7 Hz, 1H), 2.20 – 2.07 (m, 2H), 1.97 – 1.82 (m, 2H), 1.64 (s, 1H), 1.55 (dd, J = 12.4, 5.0 Hz, 1H), 1.20 (td, J = 11.9, 5.5 Hz, 1H), 1.06 (s, 3H), 0.96 (d, J = 6.9 Hz, 3H), 0.84 (d, J = 6.9 Hz, 3H). ^{13}C NMR (400 MHz, Chloroform-*d*) δ 173.31, 171.50, 170.69, 160.05, 138.49, 138.35, 138.15, 138.07, 128.54, 128.53, 128.49, 128.06, 127.99, 127.96, 127.95, 127.90, 127.83, 127.80,

125.74, 94.44, 84.92, 81.24, 75.82, 75.69, 75.12, 73.64, 71.47, 70.06, 68.24, 63.64, 63.43, 61.28, 59.77, 55.47, 55.11, 40.49, 35.79, 29.96, 29.22, 29.01, 28.09, 23.55, 17.61, 17.18, 16.84, 13.88. ESI-MS *m/z* calcd for $C_{54}H_{62}O_{14}Na$ $[M+Na]^+$ 1005.4032, found 1005.4018.

Synthesis of (5bS,6aS,7aR,8aS,9aS,9bS,10aS,10bS)-8a-iso propyl-10b-methyl-3-oxo-1,2,3,5,5b,6, 6a, 8,8a, 9a, 9b,10b-dodecahydrotris(oxireno) [2',3':4b,5; 2'',3'':6,7;2''',3''':8a,9] phenanthrol [1,2-c]furan-8-yl((3R,4S,5S,6R)-3,4,5-trihydroxy-6-(hydroxymethyl) tetrahydro-2H-pyran-2-yl) succinate (TG1). A suspension of 3 (10 mg, 0.010 mmol) and Pd/C (10%, 15 mg) in MeOH:THF (1:1, 2 mL) was stirred at RT under hydrogen gas for 3 h. The mixture was filtered by Celite, then concentrated to give a residue. The residue was purified by silica gel column chromatography (CH_2Cl_2/CH_3OH, 15:1) to give the **TG1β** (3.04 mg, 48.8%) and **TG1α** (2.50 mg, 40.2%), both as a white solid.

TG1 (β): ^{1}H NMR (400 MHz, Methanol-d_4) δ 5.49 (d, J = 7.9 Hz, 1H), 5.08 (dd, J = 4.2, 1.0 Hz, 1H), 3.96 (t, J = 2.9 Hz, 1H), 3.82 (dd, J = 12.0, 1.7 Hz, 1H), 3.68 (d, J = 1.7 Hz, 1H), 3.63 (d, J = 3.2 Hz, 1H), 3.46 (dd, J = 5.6, 3.4 Hz, 1H), 3.41 (d, J = 9.0 Hz, 1H), 3.38 – 3.34 (m, 2H), 2.80 – 2.67 (m, 4H), 2.26 (dt, J = 15.2, 5.9 Hz, 2H), 2.07 (dd, J = 19.4, 7.3 Hz, 1H), 1.96 – 1.84 (m, 2H), 1.66 – 1.55 (m, 1H), 1.51 (dd, J = 12.5, 5.2 Hz, 1H), 1.29 (d, J = 3.3 Hz, 6H), 1.04 (s, 3H), 0.94 (d, J = 6.9 Hz, 3H), 0.84 (d, J = 6.9 Hz, 3H).

TG1 (α): ^{1}H NMR (400 MHz, Methanol-d_4) δ 5.09 (d, J = 4.3 Hz, 1H), 4.69 – 4.55 (m, 1H), 3.96 (d, J = 3.2 Hz, 1H), 3.92 – 3.84 (m, 1H), 3.83 – 3.77 (m, 1H), 3.75 – 3.67 (m, 1H), 3.64 (dd, J = 9.2, 4.1 Hz, 1H), 3.60 – 3.51 (m, 1H), 3.47 (t, J = 5.1 Hz, 1H), 3.45 – 3.35 (m, 1H), 2.80 – 2.69 (m, 4H), 2.34 – 2.00 (m, 4H), 1.98 – 1.85 (m, 2H), 1.67 – 1.47 (m, 2H), 1.30 (d, J = 3.7 Hz, 3H), 1.09 (d, J = 4.2 Hz, 1H), 1.02 (d, J = 13.0 Hz, 3H), 0.94 (d, J = 6.9 Hz, 3H), 0.83 (d, J = 6.9 Hz, 3H). The ^{13}C NMR data were as described in the previous literature [28]. ESI-MS *m/z* calcd for $C_{30}H_{38}O_{14}Na$ $[M+Na]^+$ 645.2154, found 645.2170.

Synthesis of Succinic Acid Mono-((2R,4aR,7R,8R,8aR)-6,8-bis(benzyloxy)-2-phenylhexahydrop- yrano[3,2-d] [1,3]dioxin-7-yl) Ester or Succinic Acid Mono-((2R,4aR,7R,8S,8aS)-6, 7-bis(benzyloxy)-2-phenylhexahydropyrano[3,2-d][1,3] dioxin-8-yl) Ester (5). **4** (1.71 g, 3.82 mmol) dissolved in DCM–DIPEA (10:1, 11 mL) was treated with succinic anhydride (1.91 g, 19.1 mmol), stirred at RT for 24 h then eliminated the solvent. The residue was dissolved in EtOAc (40 mL), washed with brine (40 mL), saturated $NaHCO_3$ (aq), dried over $MgSO_4$ and concentrated. The residue was purified via silica gel column chromatography (CH_2Cl_2/CH_3OH, 50:1) to supply the compound **5** as a light colorless solid (1.675 g, 80%). ^{1}H NMR (400 MHz, Chloroform-*d*) δ 7.55 – 7.18 (m, 30H), 5.60 (s, 1H), 5.47 (s, 1H), 5.32 (t, J = 9.4 Hz, 1H), 5.11 (t, J = 8.4 Hz, 1H), 4.97 (d, J = 11.7 Hz, 1H), 4.86 (dd, J = 12.0, 6.9 Hz, 3H), 4.70 (dd, J = 18.1, 6.8 Hz, 3H), 4.64 (d, J = 4.8 Hz, 1H), 4.59 (d, J = 12.3 Hz, 1H), 4.53 (d, J = 7.9 Hz, 1H), 4.39 (dt, J = 10.1, 4.7 Hz, 2H), 3.90 – 3.76 (m, 3H), 3.72 (t, J = 9.1 Hz, 1H), 3.62 (t, J = 9.5 Hz, 1H), 3.57 – 3.50 (m, 2H), 3.46 (dt, J = 14.3, 4.9 Hz, 1H), 2.67 – 2.38 (m, 8H). ^{13}C NMR (400 MHz, Chloroform-*d*) δ 177.32, 170.97, 170.50, 138.14, 137.94, 137.15, 136.91, 136.86, 129.01, 128.95, 128.50, 128.41, 128.30, 128.26, 128.18, 128.12, 128.02, 127.96, 127.92, 127.89, 127.75, 127.72, 127.67, 126.06, 126.00, 103.06, 101.25, 100.15, 81.50, 79.59, 78.66, 78.34, 74.50, 74.10, 73.29, 73.09, 71.72, 70.77, 68.66, 66.23, 66.09, 28.75, 28.70, 28.65, 26.90. ESI-MS *m/z* calcd for $C_{31}H_{32}O_9Na$ $[M+Na]^+$ 571.1939, found 571.1935.

Synthesis of (2S,6R,7R,8S)-6,8-bis(benzyloxy)-2-phenylhexahydropyrano[3,2-d][1,3]dioxin-7-yl((5bS,6aS,7aR,8R,8aS,9aS,9bS, 10aS,10bS)-8a-isopropyl-10b-methyl-3-oxo-1,2,3,5,5b,6,6a,8,8a,9a,9b,10b-dodecahydrotris(oxireno)[2',3':4b,5;2'',3'':6,7;2''', 3''':8a,9]phenanthro[1,2-c]furan-8-yl) succinate or (2R,4aR,6R,7R,8S,8aR)-6,7-bis(benzyloxy)-2-phenylhexahydropyrano [3,2-d][1,3] dioxin-8-yl((5bS,6aS,7aR,8aS,9aS,9bS,10aS,10bS)-8a-isopropyl-10b-methyl-3-oxo-1,2,3,5,5b,6,6a,8,8a,9a,9b,10b-dodecahydrotris(oxireno)[2',3':4b,5;2'',3'':6,7;2''',3''':8a,9]phenanthro[1,2-c]furan-8-yl) succinate (6). To a mixture of triptolide (36 mg, 0.1 mmol), **5** (84.42 mg, 0.154 mmol), EDCI (38.34 mg, 0.2 mmol), DMAP (3.66 mg, 0.03 mmol) dissolved in dry CH_2Cl_2 (3 mL) was stirred for 20 h at RT. The resulting mixture was dissolved in CH_2Cl_2 (5 mL), washed with water (5 mL), brine (5 mL) and saturated $NaHCO_3$ (aq) (5 mL), dried over Na_2SO_4, then evaporated to provide a residue. The residue was purified through silica gel column chromatography (Cy-EtOAc, 4:1, twice) to give compounds **6-2** (41.55 mg,46.67%) and **6-3** (20.77 mg, 23.33%) as a white solid. ESI-MS *m/z* calcd for $C_{51}H_{54}O_{14}Na$ $[M+Na]^+$ 913.3411, found 913.3547.

6-2: ^{1}H NMR (400 MHz, Chloroform-*d*) δ 7.54 – 7.14 (m, 15H), 5.55 (s, 1H), 5.10 – 5.02 (m, 2H), 4.80 (dd, *J* = 20.7, 12.1 Hz, 2H), 4.66 (s, 1H), 4.64 – 4.56 (m, 2H), 4.55 – 4.48 (m, 1H), 4.35 (dd, *J* = 10.5, 5.0 Hz, 1H), 4.09 (q, *J* = 7.2 Hz, 1H), 3.85 – 3.75 (m, 2H), 3.75

– 3.67 (m, 1H), 3.49 (d, *J* = 3.1 Hz, 1H), 3.40 (dd, *J* = 13.4, 5.2 Hz, 2H), 2.68 – 2.45 (m, 4H), 2.34 – 2.23 (m, 1H), 2.15 – 2.05 (m, 1H), 2.01 (s, 2H), 1.94 – 1.86 (m, 1H), 1.82 (d, *J* = 14.9 Hz, 1H), 1.54 (dd, *J* = 11.8, 4.3 Hz, 1H), 1.22 (s, 2H), 1.03 (s, 3H), 0.91 (d, *J* = 6.9 Hz, 3H), 0.80 (d, *J* = 6.9 Hz, 3H). ^{13}C NMR (400 MHz, $CDCl_3$) δ 173.55, 171.94, 170.72, 160.28, 138.51, 137.52, 137.28, 129.35, 128.81, 128.61, 128.59, 128.39, 128.32, 128.13, 128.00, 126.31, 125.93, 101.55, 100.56, 81.75, 78.57, 74.39, 73.70, 71.48, 71.17, 70.27, 69.01, 66.58, 63.83, 63.70, 61.53, 60.73, 60.04, 55.73, 55.29, 40.67, 36.01, 30.19, 29.31, 28.26, 23.77, 21.39, 17.83, 17.39, 17.04, 14.53, 14.13.

6-3: ^{1}H NMR (400 MHz, Chloroform-*d*) δ 7.56 – 7.15 (m, 15H), 5.46 (s, 1H), 5.36 – 5.25 (m, 1H), 5.06 (s, 1H), 4.95 (d, *J* = 11.7 Hz, 1H), 4.81 (d, *J* = 11.6 Hz, 1H), 4.74 – 4.60 (m, 4H), 4.37 (dd, *J* = 10.5, 4.9 Hz, 1H), 4.12 (q, *J* = 7.1 Hz, 1H), 3.84 – 3.72 (m, 2H), 3.62 (t, *J* = 9.6 Hz, 1H), 3.57 – 3.49 (m, 1H), 3.46 (d, *J* = 4.1 Hz, 1H), 3.41 (d, *J* = 5.6 Hz, 1H), 2.74 – 2.52 (m, 4H), 2.38 – 2.26 (m, 1H), 2.11 (dt, *J* = 14.8, 5.8 Hz, 2H), 2.04 (s, 1H), 1.92 – 1.78 (m, 1H), 1.69 – 1.50 (m, 2H), 1.26 (d, *J* = 1.6 Hz, 2H), 1.04 (s, 3H), 0.92 (d, *J* = 7.0 Hz, 3H), 0.80 (d, *J* = 6.9 Hz, 3H). ^{13}C NMR (101 MHz, $CDCl_3$) δ 173.56, 171.89, 171.22, 160.28, 138.33, 137.31, 137.23, 129.38, 128.83, 128.64, 128.61, 128.55, 128.37, 128.31, 128.10, 126.53, 125.93, 103.39, 101.77, 79.96, 79.01, 74.86, 73.44, 72.05, 71.43, 70.28, 69.06, 66.39, 63.81, 63.68, 61.49, 60.01, 55.72, 55.26, 40.67, 36.00, 31.77, 30.52, 30.03, 29.37, 29.29, 28.29, 23.74, 17.81, 17.40, 17.04, 14.53, 14.12.

Synthesis of (5bS,6aS,7aR,8R,8aS,9aS,9bS,10aS,10bS)-8a-isopropyl-10b-methyl-3-oxo-1,2,3,5, 5b,6, 6a,8, 8a, 9a,9b,10b-dodecahydrotris(oxireno) [2',3':4b,5; 2'', 3'':6,7;2''',3''':8a,9] phenanthro[1,2-c]furan-8-yl ((2R,3R,4S,5S,6R)-2,4,5-trihydroxy-6-(hydroxymethyl) tetrahydro-2H-pyran-3-yl) succinate (TG2). A suspension of **6-2** (10 mg, 0.010 mmol) and Pd/C (10%, 15 mg) in MeOH:THF (1:1, 2 mL) was stirred at RT under hydrogen gas for 3 h. The mixture was filtered by Celite, then concentrated to give a residue. The residue was purified by silica gel column chromatography (CH_2Cl_2/CH_3OH, 15:1) to give the compound **TG2** (5.79 mg, 93%) as a white solid. ^{1}H NMR (600 MHz, Methanol-d_4) δ 5.09 (d, *J* = 7.5 Hz, 1H), 4.68 – 4.51 (m, 1H), 3.96 (s, 1H), 3.87 (dt, *J* = 22.5, 8.6 Hz, 1H), 3.83 – 3.75 (m, 1H), 3.73 – 3.64 (m, 1H), 3.63 (s, 1H), 3.56 – 3.44 (m, 2H), 3.38 (dt, *J* = 19.5, 9.6 Hz, 1H), 2.83 – 2.67 (m, 4H), 2.30 – 2.17 (m, 2H), 2.15 – 2.00 (m, 1H), 1.91 (dd, *J* = 17.0, 10.3 Hz, 2H), 1.51 (dd, *J* = 12.6, 5.4 Hz, 1H), 1.37 – 1.23 (m, 5H), 1.04 (s, 3H), 0.94 (d, *J* = 6.5 Hz, 3H), 0.83 (d, *J* = 6.9 Hz, 3H). ^{13}C NMR (600 MHz, Methanol-d_4) δ 174.70, 172.27, 162.48, 129.46, 124.14, 94.84, 92.51, 89.78, 76.81, 75.73, 74.48, 71.68, 71.54, 70.59, 62.87, 61.35, 59.68, 55.41, 54.81, 40.05, 35.41, 29.43, 28.82, 28.49, 28.33, 27.80, 26.70, 22.76, 16.51, 12.78. ESI-MS *m/z* calcd for $C_{30}H_{38}O_{14}Na$ $[M+Na]^+$ 645.2154, found 645.2170.

Synthesis of (5bS,6aS,7aR,8aS,9aS,9bS,10aS,10bS)-8a-isopropyl-10b-methyl-3-oxo-1,2,3,5, 5b,6, 6a,8,8a,9a, 9b,10b-dodecahydrotris(oxireno) [2',3':4b,5;2'', 3'':6,7;2''',3''': 8a,9] phenanthro[1,2-c]furan-8-yl ((3R,4S,5R,6R)-2,3,5-trihydroxy-6-(hydroxymethyl) tetrahydro- 2H-pyran-4-yl) succinate (TG3). A suspension of **6-3** (10 mg, 0.010 mmol) and Pd/C (10%, 15 mg) in MeOH:THF (1:1, 2 mL) was stirred at RT under hydrogen gas for 3 h. The mixture was filtered by Celite, then concentrated to give a residue. The residue was purified by silica gel column chromatography (CH_2Cl_2/CH_3OH, 15:1) to give the compound **TG3** (5.91 mg, 95%) as a white solid. ^{1}H NMR (600 MHz, Methanol-d_4) δ 5.34 (t, *J* = 5.1 Hz, 1H), 5.08 (d, *J* = 6.8 Hz, 1H), 4.68 – 4.61 (m, 1H), 4.57 (d, *J* = 7.0 Hz, 1H), 3.96 (d, *J* = 3.1 Hz, 1H), 3.93 – 3.77 (m, 1H), 3.73 – 3.61 (m, 2H), 3.56 – 3.44 (m, 1H), 2.81 – 2.65 (m, 4H), 2.32 – 2.14 (m, 3H), 2.03 (q, *J* = 6.6 Hz, 1H), 1.97 – 1.86 (m, 1H), 1.64 – 1.56 (m, 1H), 1.50 (dd, *J* = 12.6, 5.4 Hz, 1H), 1.29 (d, *J* = 5.7 Hz, 5H), 1.04 (s, 3H), 0.94 (d, *J* = 7.0 Hz, 3H), 0.83 (d, *J* = 7.0 Hz, 3H). ^{13}C NMR (400 MHz, Methanol-d_4) δ 176.08, 173.42, 163.89, 130.84, 125.51, 96.22, 91.15, 78.18, 75.85, 73.04, 72.92, 72.09, 71.99, 71.78, 64.26, 62.73, 62.72, 62.56, 56.18, 41.43, 36.79, 30.82, 29.17, 24.41, 24.15, 23.74, 17.90, 17.12, 14.18. ESI-MS *m/z* calcd for $C_{30}H_{38}O_{14}Na$ $[M+Na]^+$ 645.2154, found 645.2167.

Synthesis of Succinic Acid Mono-((2R,3R,4S,5R,6R)-4,5,6-tris(benzyloxy)-2-((benzyloxy) methyl) tetrahydro-2H-pyran-3-yl) Ester (8). 7 (0.697 g, 1.291 mmol) dissolved in DCM–DIPEA (10:1, 11 mL) was dealt with succinic anhydride (645.5 mg, 6.455 mmol), stirred at RT for 16 h. The solvent was then evaporated. The residue was dissolved in EtOAc (20 mL), washed with brine, saturated $NaHCO_3$ (aq), dried over $MgSO_4$ and concentrated. The residue was purified by silica gel column chromatography (CH_2Cl_2/CH_3OH, 50:1) to attain the compound **8** as a light colorless solid (715.8 mg, 86.6%). ^{1}H NMR (400 MHz, Chloroform-*d*) δ 7.41 – 7.21 (m, 20H, Ar-H), 5.05 – 4.91 (m, 3H), 4.81 (d, J = 11.6 Hz, 1H), 4.70 (dd, J = 11.4, 7.4 Hz, 2H), 4.61 (d, J = 11.6 Hz, 1H), 4.58 – 4.50 (m, 3H), 3.65 – 3.51 (m, 5H), 2.55 – 2.25 (m, 4H). ^{13}C NMR (400 MHz, Chloroform-*d*) δ 177.61, 171.07, 138.54, 138.34, 138.13, 137.33, 128.58, 128.49,

128.48, 128.45, 128.32, 128.16, 127.99, 127.97, 127.93, 127.86, 127.82, 127.75, 102.39, 82.14, 81.85, 75.22, 75.09, 73.73, 73.47, 71.51, 71.30, 69.84, 28.79, 28.67. ESI-MS *m/z* calcd for $C_{38}H_{40}O_9Na$ $[M+Na]^+$ 663.2565, found 663.2566.

Synthesis of (5bS,6aS,7aR,8aS,9aS,9bS,10aS,10bS)-8a-isopropyl-10b-methyl-3-oxo-1,2,3,5,5b,6,6a, 8,8a,9a,9b,10b-dodecahydrotris(oxireno)[2',3':4b,5;2'',3'': 6,7;2''',3''':8a,9] phenanthrol[1,2-c] furan-8-yl ((2R, 3R,4S,5R,6R)-4,5,6-tris (benzyloxy)-2-((benzyloxy) methyl)tetrahydro-2H-pyran-3-yl) succinate (9). To a mixture of triptolide (36 mg, 0.1 mmol), **8** (89.64 mg, 0.14 mmol), EDCI (38.34 mg, 0.1 mmol), DMAP (3.66 mg, 0.03 mmol) dissolved in dry CH_2Cl_2 (3 mL) was stirred for 18 h at RT. The resulting combination was dissolved in CH_2Cl_2 (5 mL), washed with water (5 mL), brine (5 mL) and saturated $NaHCO_3$ (aq) (5 mL), dried over Na_2SO_4, then evaporated to provide a residue. The residue was purified through silica gel column chromatography (Cy-EtOAc, 3:1, twice) to give the compounds **9** as a white solid (66.8 mg, 68%). ^{1}H NMR (400 MHz, Chloroform-*d*) δ 7.40 – 7.18 (m, 20H), 5.03 (s, 1H), 5.00 – 4.88 (m, 3H), 4.80 (d, J = 11.7 Hz, 1H), 4.67 (dd, J = 11.4, 4.5 Hz, 2H), 4.61 (d, J = 3.2 Hz, 3H), 4.52 (d, J = 5.1 Hz, 2H), 4.51 – 4.47 (m, 1H), 3.78 (d, J = 3.2 Hz, 1H), 3.65 – 3.58 (m, 1H), 3.58 – 3.51 (m, 3H), 3.49 (d, J = 3.0 Hz, 1H), 3.37 (d, J = 5.6 Hz, 1H), 2.63 (d, J = 10.3 Hz, 1H), 2.58 – 2.52 (m, 2H), 2.51 – 2.42 (m, 1H), 2.34 – 2.23 (m, 2H), 2.05 (dt, J = 14.8, 5.8 Hz, 2H), 1.87 (p, J = 6.9 Hz, 1H), 1.83 – 1.74 (m, 1H), 1.63 (s, 1H), 1.53 (dd, J = 12.4, 5.0 Hz, 1H), 1.17 (td, J = 12.0, 5.7 Hz, 1H), 1.00 (s, 3H), 0.90 (d, J = 7.0 Hz, 3H), 0.79 (d, J = 6.9 Hz, 3H). ^{13}C NMR (400 MHz, Chloroform-*d*): δ (ppm) 173.15, 171.69, 170.84, 159.85, 138.54, 138.21, 137.19, 128.40, 128.32, 128.30, 128.16, 127.98, 127.81, 127.77, 127.72, 127.61, 127.59, 127.58, 102.14, 82.04, 81.91, 75.14, 74.91, 73.59, 73.53, 71.15, 71.06, 70.98, 69.89, 69.58, 63.48, 63.29, 61.17, 59.63, 55.35, 54.94, 40.30, 35.63, 29.80, 28.86, 27.93, 23.36, 17.44, 17.02, 16.63, 13.74. ESI-MS *m/z* calcd for $C_{58}H_{62}O_{14}Na$ $[M+Na]^+$ 1005.4032, found 1005.4038.

Synthesis of (5bS,6aS,7aR,8aS,9aS,9bS,10aS,10bS)-8a-isopropyl-10b-methyl-3-oxo-1,2,3,5,5b,6, 6a,8,8a, 9a, 9b,10b-dodecahydrotris(oxireno) [2',3':4b,5; 2'', 3'':6,7;2''',3''':8a,9] phenanthrol [1,2-c]furan-8-yl ((2R,4R,5R,6R)-4,5,6-trihydroxy-2-(hydroxymethyl) tetrahydro-2H-pyran-3-yl) succinate (TG4). A suspension of **9** (10 mg, 0.010 mmol) and Pd/C (10%, 15 mg) in MeOH:THF (1:1, 2 mL) was stirred at RT under hydrogen gas for 3 h. The mixture was filtered through Celite, then concentrated to provide a residue. The residue was purified by silica gel column chromatography (CH_2Cl_2/CH_3OH, 15:1) to give the compound **TG4** (5.72 mg, 92%) as a white solid. ^{1}H NMR (400 MHz, Methanol-d_4) δ 5.14 – 5.07 (m, 1H), 4.77 – 4.67 (m, 1H), 4.01 – 3.93 (m, 1H), 3.87 (t, J = 9.4 Hz, 1H), 3.67 – 3.55 (m, 2H), 3.47 (qd, J = 9.6, 3.5 Hz, 3H), 3.31 (t, J = 1.8 Hz, 2H), 2.80 – 2.66 (m, 4H), 2.33 – 2.20 (m, 2H), 2.16 – 2.00 (m, 1H), 1.91 (dq, J = 14.6, 7.0 Hz, 2H), 1.62 – 1.47 (m, 1H), 1.30 (d, J = 3.8 Hz, 4H), 1.04 (s, 3H), 0.95 (d, J = 6.9 Hz, 3H), 0.84 (d, J = 6.8 Hz, 3H). ^{13}C NMR (400 MHz, Methanol-d_4) δ 176.06, 173.66, 163.91, 125.49, 98.23, 93.74, 76.25, 73.74, 73.48, 72.96, 72.39, 71.99, 70.82, 64.86, 64.25, 62.83, 60.99, 56.79, 56.20, 41.42, 36.78, 30.81, 30.74, 30.06, 29.25, 29.21, 24.14, 17.91, 17.07, 14.23. ESI-MS *m/z* calcd for $C_{30}H_{38}O_{14}Na$ $[M+Na]^+$ 645.2154, found 645.2165.

Synthesis of Benzyl 2,3,4,6-tetra-O-benzyl-D-glucopyranoide (10) [48]**.** To a combination of D-glucose (0.9 g, 5 mmol), NaH (0.6 g of 60% dispersion in mineral oil, 15 mmol) in dry DMF was kept at RT for 30 min, then cooled to 0 ℃. The mixture was added BnBr (2.15 mL, 17.5 mmol) dropwise over 5 min, and maintained for 10 min, then stirred at RT for 2.5 h. The mixture was added the same quantities of NaH and BnBr in the same process. After an additional 2.5 h, NaH (2 eq, 0.4 g, 10 mmol) and BnBr (1.9 eq, 1.2 mL, 9.5 mmol) were added continuously. The reaction mixture was stirred overnight, then added ice water (1 mL) slowly to eliminate the extra NaH. The mixture was evaporated to remove the solvent, diluted with CH_2Cl_2 (25 mL), washed with water (25 mL) and brine (25 mL), dried over $MgSO_4$, and concentrated to obtain a residue. The crude residue was purified by silica gel column chromatography (Cy-EtOAc 8:1) to give the compound **10** (1.9 g, 60.3%) as a white solid. ^{1}H NMR (400 MHz, Chloroform-*d*) δ 7.43 – 7.23 (m, 23H), 7.21 – 7.13 (m, 2H), 5.03 – 4.91 (m, 3H), 4.82 (dd, J = 16.6, 10.9 Hz, 2H), 4.77 – 4.66 (m, 2H), 4.64 (s, 1H), 4.62 – 4.55 (m, 2H), 4.55 – 4.50 (m, 1H), 3.78 (dd, J = 10.8, 2.1 Hz, 1H), 3.75 – 3.68 (m, 1H), 3.67 – 3.59 (m, 2H), 3.57 – 3.51 (m, 1H), 3.49 (ddd, J = 9.5, 4.7, 2.0 Hz, 1H). ^{13}C NMR spectrum is in agreement with those published.[48] ESI-MS *m/z* calcd for $C_{41}H_{42}O_6Na$ $[M+Na]^+$ 653.2879, found 653.2968.

Synthesis of Benzyl 6-O-acetyl-2,3,4-tri-O-benzyl-D-glucopyranoside (11). A mixture of zinc chloride (546 mg, 4 mmol) in HOAc–Ac_2O (1:5, 6 mL) was cooled to 0 ℃. Then **10** (488 mg, 0.77 mmol) dissolved in HOAc–Ac_2O (1:5, 6 mL) was added slowly to the suspension at 0 ℃. The reaction mixture was kept at RT for 1.5 h, and recrystallized with ice water (20 mL) to afford the light-brown precipitation. The precipitation was washed with water and purified by silica gel column chromatography (Cy-EtOAc 15:1) to give the compound **11** (246.58 mg, 55%) as a light white solid. ^{1}H NMR (400 MHz, Chloroform-*d*) δ 7.43 – 7.25 (m, 22H), 5.02 – 4.93 (m, 3H),

4.89 (d, J = 10.9 Hz, 1H), 4.81 (d, J = 10.9 Hz, 1H), 4.75 (d, J = 10.9 Hz, 1H), 4.69 (d, J = 11.9 Hz, 1H), 4.60 (d, J = 10.8 Hz, 1H), 4.54 (d, J = 7.8 Hz, 1H), 4.40 (dd, J = 11.9, 1.9 Hz, 1H), 4.27 (dd, J = 11.9, 4.7 Hz, 1H), 3.70 (t, J = 8.7 Hz, 1H), 3.62 – 3.49 (m, 3H), 2.09 (s, 3H, $COCH_3$). ESI-MS *m/z* calcd for $C_{36}H_{38}O_7Na$ $[M+Na]^+$ 605.2515, found 605.2595.

Synthesis of Benzyl 2,3,4-tri-O-benzyl- D-glucopyranoside (12). 11 (353 mg, 0.605 mmol) dissolved in 0.025 M NaOMe (5 mL) was stirred at RT for 5 h. The ice water (20 mL) was poured into the reaction mixture and stirred for 30 min to afford a white precipitation. The resulting precipitate was washed with saturated $NaHCO_3$ (aq), water, dried over Na_2SO_4 and concentrated to provide a crude residue. The crude residue was purified by silica gel column chromatography (Cy-EtOAc 10:1) to give the compound **12** (297.43 mg, 91%) as a light white solid. ^{1}H NMR (400 MHz, Chloroform-*d*) δ 7.41 – 7.28 (m, 20H), 4.99 – 4.56 (m, 10H), 3.88 (dd, J = 11.9, 2.7 Hz, 1H), 3.76 – 3.65 (m, 2H), 3.58 (t, J = 9.3 Hz, 1H), 3.50 (dd, J = 9.0, 7.9 Hz, 1H), 3.38 (ddd, J = 9.6, 4.6, 2.8 Hz, 1H). ESI-MS *m/z* calcd for $C_{34}H_{36}O_6Na$ $[M+Na]^+$ 563.2410, found 563.2457.

Synthesis of Succinic Acid Mono-((2R,3R,4S,5R)-3,4,5,6-tetrakis(benzyloxy) tetrahydro-2H- pyran-2-yl) methanol) Ester (13). 12 (0.697 g, 1.291 mmol) dissolved in DCM–DIPEA (10:1, 16.5 mL) was handled with succinic anhydride (1.301 g, 6.455 mmol), stirred at RT for 16 h then the solvent was evaporated. The residue was dissolved in EtOAc (20 mL), washed with brine (20 mL), saturated $NaHCO_3$ (aq), dried over $MgSO_4$ and concentrated. The residue was purified by silica gel column chromatography (CH_2Cl_2/CH_3OH, 50:1) to acquire the compound **13** as a light colorless solid (1.499 g, 90%). ^{1}H NMR (400 MHz, Chloroform-*d*) δ 7.44 – 7.16 (m, 20H), 4.98 – 4.90 (m, 2H), 4.82 (dd, J = 26.6, 10.8 Hz, 2H), 4.72 (d, J = 10.9 Hz, 1H), 4.65 (d, J = 11.9 Hz, 1H), 4.60 – 4.49 (m, 2H), 4.41 (dd, J = 11.8, 2.0 Hz, 1H), 4.27 (dd, J = 11.8, 4.5 Hz, 1H), 4.20 – 4.09 (m, 1H), 3.71 – 3.62 (m, 1H), 3.58 – 3.46 (m, 3H), 2.66 – 2.58 (m, 4H), 2.05 (s, 1H), 1.26 (t, J = 7.1 Hz, 2H). ESI-MS *m/z* calcd for $C_{38}H_{40}O_9Na$ $[M+Na]^+$ 663.2565, found 663.2566.

Synthesis of (5bS,6aS,7aR,8aS,9aS,9bS,10aS,10bS)-8a-isopropyl-10b-methyl-3-oxo-1,2,3,5, 5b, 6, 6a, 8,8a, 9a, 9b,10b-dodecahydrotris(oxireno) [2',3':4b,5;2'',3'': 6,7;2''', 3''':8a,9] phenanthro[1,2-c]furan-8-yl (((2R,3R,4S,5R)-3,4,5,6-tetrakis (benzyloxy)tetrahydro- 2H-pyran-2-yl)methyl) succinate (14). To a mixture of triptolide (36 mg, 0.1 mmol), **13** (89.64 mg, 0.14 mmol), EDCI (38.34 mg, 0.2 mmol), DMAP (3.66 mg, 0.03 mmol) dissolved in dry CH_2Cl_2 (3 mL) was stirred for 18 h at RT. The resulting mixture was dissolved in CH_2Cl_2 (5 mL), washed with water (5 mL), brine (5 mL) and saturated $NaHCO_3$ (aq) (5 mL), dried over Na_2SO_4, then evaporated to provide a residue. The residue was purified by silica gel column chromatography (Cy-EtOAc, 3:1, twice) to attain the compounds **14** as a white solid (73.39 mg, 74.7%). ^{1}H NMR (400 MHz, Chloroform-*d*) δ 7.40 – 7.24 (m, 20H), 5.06 (d, J = 3.7 Hz, 1H), 4.99 – 4.91 (m, 2H), 4.87 (d, J = 10.8 Hz, 1H), 4.80 (d, J = 10.9 Hz, 1H), 4.75 – 4.67 (m, 2H), 4.67 – 4.59 (m, 2H), 4.57 (s, 1H), 4.52 (d, J = 7.7 Hz, 1H), 4.40 (dd, J = 11.8, 2.1 Hz, 1H), 4.31 (dd, J = 11.8, 4.6 Hz, 1H), 3.80 (d, J = 3.1 Hz, 1H), 3.66 (t, J = 8.7 Hz, 1H), 3.61 – 3.54 (m, 1H), 3.54 – 3.49 (m, 2H), 3.39 (d, J = 5.6 Hz, 1H), 2.79 – 2.63 (m, 4H), 2.31 (d, J = 17.6 Hz, 1H), 2.08 (dt, J = 14.7, 5.6 Hz, 2H), 1.94 – 1.78 (m, 2H), 1.65 – 1.50 (m, 4H), 1.19 (td, J = 12.1, 5.7 Hz, 1H), 1.03 (d, J = 4.4 Hz, 3H), 0.93 (d, J = 6.9 Hz, 3H), 0.83 (d, J = 6.9 Hz, 3H). ^{13}C NMR (400 MHz, Chloroform- *d*) δ 173.33, 171.98, 171.77, 160.06, 138.59, 138.44, 138.03, 137.38, 128.58, 128.54, 128.50, 128.27, 128.16, 128.02, 127.84, 127.82, 125.73, 102.60, 84.85, 82.36, 75.87, 75.16, 75.04, 73.06, 71.38, 71.34, 70.07, 63.64, 63.45, 61.26, 59.78, 55.47, 55.13, 40.48, 35.78, 29.97, 29.24, 29.12, 28.19, 23.53, 17.61, 17.19, 16.84, 13.90. ESI-MS *m/z* calcd for $C_{54}H_{62}O_{14}Na$ $[M+Na]^+$ 1005.4032, found 1005.4038.

Synthesis of (5bS,6aS,7aR,8aS,9aS,9bS,10aS,10bS)-8a-isopropyl-10b-methyl-3-oxo-1,2,3,5,5b,6, 6a, 8,8a, 9a, 9b,10b-dodecahydrotris(oxireno)[2',3':4b,5;2'', 3'':6,7;2''',3''':8a,9] phenanthrol[1,2-c] furan-8-yl (((2R,3S,4S,5R)-3,4,5,6-tetrah-ydroxytetrahydro-2H-pyran-2-yl)methyl) succinate (TG6). A suspension of **14** (10 mg, 0.010 mmol) and Pd/C (10%, 15 mg) in MeOH:THF (1:1, 2 mL) was stirred at RT under hydrogen gas for 3 h. The combination was filtered via Celite, then concentrated to give a residue. The residue was purified by silica gel column chromatography (CH_2Cl_2/CH_3OH, 15:1) to give the compound **TG6** (5.54 mg, 89%) a white solid white. ^{1}H NMR (400 MHz, Methanol-d_4) δ 5.08 (d, *J* = 8.2 Hz, 1H), 4.81 (dd, *J* = 9.6, 1.9 Hz, 1H), 4.51 – 4.34 (m, 1H), 4.19 (ddd, *J* = 14.9, 11.8, 6.0 Hz, 1H), 4.01 – 3.93 (m, 1H), 3.70 – 3.62 (m, 1H), 3.53 – 3.44 (m, 1H), 3.36 (dd, *J* = 9.3, 3.2 Hz, 1H), 2.70 (q, *J* = 3.6, 2.7 Hz, 4H), 2.30 – 2.16 (m, 2H), 2.14 – 1.99 (m, 2H), 1.96 – 1.85 (m, 2H), 1.61 (q, *J* = 7.8, 6.2 Hz, 1H), 1.51 (dd, *J* = 12.3, 5.4 Hz, 1H), 1.30 (q, *J* = 3.8 Hz, 5H), 1.04 (s, 3H), 0.94 (d, *J* = 6.9 Hz, 3H), 0.83 (d, *J* = 6.9 Hz, 3H). ^{13}C NMR (400 MHz, Methanol-d_4) δ 176.09, 173.92, 163.89, 130.85, 125.52, 121.55, 98.24, 93.97, 75.32, 74.74, 73.75, 73.05, 71.98, 70.60, 64.87, 64.26, 62.69, 61.00, 56.74, 56.18,

41.45, 36.79, 30.83, 30.33, 30.06, 29.10, 28.10, 24.16, 17.87, 17.08, 14.19. ESI-MS *m/z* calcd for $C_{30}H_{38}O_{14}Na$ $[M+Na]^+$ 645.2154, found 645.2154.

4.2. Measurement of octanol-water partition coefficient (log *P*)

3.0 mg of compound (TGs or triptolide) was dissolved in 0.5 mL of n-octanol (saturated with PBS) in a 1.5 mL tube. The tube was placed on the rotator at room temperature for 24 h, then centrifuged at 12,000 rpm/min for 5 min, 0.4 mL of the supernatant was taken out and mixed with 0.4 mL of PBS (saturated with n-octanol). The mixture was placed on a rotator for 24 h at room temperature, then centrifuged for 10 min at 12000 rpm/min, to separate the organic phase and water phase from the mixture. The concentration of the compound was measured with liquid chromatography and mass spectrometry, the peak areas of compound in water and n-octanol phase were quantified. According to the standard curve equation of the peak area and concentration of the compound, the corresponding concentration of the compound in the upper ($C_{n\text{-}octanol}$) and in the lower (C_{water}) was calculated and then calculated log*P* = log ($C_{n\text{-}octanol}/C_{water}$).

4.3. Docking analysis

To predict the interaction between D-glucose and Glut-1, molecular docking of D-glucose with Glut-1 was carried out using the crystal structure of human Glut-1 (PDB ID: 5EQH) provided by K. Kapoor [31]. Before performing ligand docking, remove substructures, add hydrogen, analyze selected structure, then adopted Multi-Channel Surface Mode to search for the binding pocket of residue selection surface 1 and to generate the protomol of the Glut-1. Then the energy minimized structure of D-glucose was subjected to SurflexDock program in SYBYL-X 2.0 version. The situation was subjected to visual analysis using PyMOL 1.7.6 software. The docking situation was evaluated by the quantity of hydrogen bonds which represent the affinity between the ligand and Glut-1.

4.4. Cell lines and cell culture

PC-9, A549, NCI-H460 and NCI-H1975 (lung carcinoma cell), DLD-1, SW620, HT29 and HCT116 (colon carcinoma cell), MCF-7, MDA-MB-231 (breast carcinoma cell) were maintained in RPMI 1640 medium supplemented with 10% fetal bovine serum (FBS, PVN) and 1% penicillin/streptomycin (100 mg/mL each). HUVEC (Human umbilical cord vein endothelial cell line), HaCaT, Rhek-1A (Human immortal keratinocyte cell line), LO2 (Human normal liver cells) were maintained in Dulbecco's Modified Eagle's Medium (DMEM) supplemented with 10% fetal bovine serum (FBS, PVN) and 1% penicillin/streptomycin (100 mg/mL each). Cells were cultivated in a humidified atmosphere at 37 °C containing 5% CO_2.

4.5. Cytotoxicity assays

Cells (4000/well in 180 μL medium) were cultured in a 96-well plate and incubated overnight, treated with different concentrations of TGs or triptolide or vehicle (DMSO) for 72 h. Then added 20 μL/well of 5 mg/mL MTT solution, proceed to incubate for 4 h. 100~150 μL DMSO was added to dissolve the resulting purple formazan crystals. The absorbance of the solution in each well was measured at 570 nm (OD value) using a BioTek Synergy HT multi-detection microplate plate reader. The IC_{50} values were calculated using the GraphPad Prism version 8.0 (GraphPad Software, San Diego, CA).

4.6. Apoptosis assays

Apoptosis was detected by an Annexin V-FITC/PI Apoptosis Detection Kit (Elabscience). The experiment was processed according to the manufacture's protocol. Briefly, untreated and treated cells were suspended in 1 × annexin binding buffer (200 μL), 5 μL APC-annexin V and 5 μL PI (10 μg/mL) were added to each sample and incubated in the dark for 20 min. After discarding the supernatant, the sample was washed with 1% BSA DPBS, then resuspend the sample in 1× annexin binding buffer, store at 4 °C. Subsequently, samples were attained on a BD FACS Canto II flow cytometer and per sample was acquired 10, 000 events. Cell populations were analyzed using the software FlowJo v10.5.3. Experiments were executed by three independent samples.

4.7. Western blotting assay

Cells were harvested by trypsinization, washed with PBS, lysed with NP-40 lysis buffer (50 mmol/L Tris pH 8.0, 150 mmol/L NaCl, and 1% NP-40) on ice, and centrifuged at 12,000 rpm for 15 min. The supernatants were collected and the protein concentration was determined

with BCA protein assay kit (Beyotime). Protein samples were separated by SDS-PAGE and transported onto polyvinylidene difluoride (PVDF) (BioRad, Hercules, CA, USA), and blocked with 5% skimmed milk. The membrane proteins were incubated using primary antibodies for Glut-1 (Abcam, 1:10000), RNA Pol II (Santa Cruz, 1:1000), GAPDH (Abcam, 1:1000), followed through incubation with anti-rabbit IgG-HRP (Abcam, 1:5000), anti-mouse IgG-HRP (Abcam, 1:5000), and enhanced chemiluminescence (GE Healthcare). Imaging and quantification of protein bands were evaluated with ImageJ software.

4.8. Knockdown and overexpression of Glut-1 gene

The lentivirus using for knockdown or overexpression of Glut-1 was purchased from Geenchem (China). The experiment was processed according to the manufacture's protocol. Briefly, cells were infected with the lentivirus containing Glut-1 knockdown or overexpression sequences for 12 h, replaced fresh medium and cultured for 72 h, and then added puromycin to screening successfully transfected cells. The selection process with puromycin was persisted for 14 days with medium replacement every two days. The expression of Glut-1 protein in knockdown or overexpression cells was measured by Western blotting. Experiments were carried out at least three times.

4.9. Mitochondrial membrane potential measurement

Mitochondrial membrane potential was detected via TMRE-Mitochondrial Membrane Potential Assay Kit (Abcam). The experiment was processed in accordance with the manufacturer's protocol. Briefly, untreated and treated cells were suspended in 1% BSA DPBS (200 μL), 0.02 μL TMRE (1 mM) were added to each sample and incubated in the dark for 20 min. After discarding the supernatant, the sample was washed with 1% BSA DPBS, then resuspend the sample in 1% BSA DPBS, store at 4 ℃. Subsequently, Samples were attained on a BD FACS Canto II flow cytometer and each sample was acquired 10, 000 events. Cell populations were analyzed using the software FlowJo v10.5.3. Experiments were performed by three independent samples.

4.10. ROS level measurement

Cell ROS level was detected by ROS detection kit (Beyotime). The experiment was processed according to the manufacture's protocol. Briefly, untreated and treated cells were suspended in 1% BSA DPBS (200 μL), 0.2 μL DCFH-DA (10 mM) were added to each sample and incubated in the dark for 30 min. After discarding the supernatant, the sample was wash with 1% BSA DPBS, then resuspend the sample in 1% BSA DPBS, store at 4 ℃. Subsequently, samples were attained on a BD FACS Canto II flow cytometer and each sample was acquired 10, 000 events. Cell populations were analyzed using the software FlowJo v10.5.3. Experiments were executed by three independent samples.

4.11. Antitumor effect *in vivo* and histopathological study

Xenografts of NCI-H1975 cells were established by subcutaneous injection into the BALB/c nude mice. Briefly, cells at the logarithmic growth phase (2×10^7/0.2 mL/mouse) were inoculated into axillary subcutaneous of BALB/c nude mice (male, 5-6 weeks, 18-22 g, purchased from GemPharmatech. Co. Ltd). When the tumor volume reached to 80 mm^3, the mice were randomized into five groups by tumor size and received various treatments: (a) Normal saline (intraperitoneal injection (ip), qd, d1-d5/week×2); (b) paclitaxel (15 mg/kg, ip, q3d×6); (c) TPL (0.2 mg/kg, ip, qd, d1-d5/week×2); (d) TG2 (1 mg/kg, ip, qd, d1-d5/week×2); (e) TG2 (2 mg/kg, ip, qd, d1-d5/week×2). The body weights of the animals, tumor's long diameter (L) and short diameter (W) were recorded every 3 days, and tumor volume (V) was calculated in accordance to the following formula: $V=L\times W^2/2$.

At the end of the observation, the mice were euthanized and tumors were excised and weighed. The curves of tumor growth was drawn according to tumor volume and days after treatment. The samples of heart, lung, liver, kidney and testis tissue were collected from mice of each group. Samples were fixed with formaldehyde, dehydrated with graded alcohol and xylene, embedded in paraffin, sectioned, and then stained with hematoxylin and eosin (H&E). Pathological injury evaluations of heart, lung, liver, kidney and testis were performed under a light microscope (Zeiss, Germany). The tumor weight inhibition (TI) was calculated according to the following formula:

$$TI\ (\%)=1-\frac{\text{Mean tumor weight of experimental group}}{\text{Mean tumor weight of control group}}\times 100$$

4.12. Pharmacokinetic study

BALB/c nude mice (male, 6-7 weeks, 22-26 g, purchased from GemPharmatech. Co. Ltd) were administrated by intravenous injection of TG2 (1 mg/kg). After intravenous injection 10, 20, 30, 60, 120 and 180 min, blood samples were collected via orbital venous plexus from 3 mice in each time point, and then centrifuged to gain plasma. The plasma was added methanol to precipitate protein, condensed the supernatant, then reconstituted with methanol. The concentration was determined through HPLC. The eluent was monitored at 220 nm. DAS 3.0 software (Shanghai, China) was used for calculating pharmacokinetic parameters.

4.13. Stability of TG2 in serum

15 μM TG2 was incubated with mice or Human serum at 37 °C for different time (0, 0.5, 1, 8, 12, 18, 60 and 72 h), then stored the sample at -80 °C. The 200 μL methanol was added into the serum samples to precipitate protein, then vortexed and ultrasound for 5 min. The chromatograms were taken by HPLC and detected at 220 nm. All the experiments were in duplicate.

4.14. Distribution of TG2 in major organs and tumor tissue

NCI-H1975 tumor-bearing mice were established according to 4.11, when the tumor volume reached approximately 500 mm^3, the mice were randomized into 3 groups (3 mice for each group). Prior to the experiments, the mice fasted for 12 h with free access to water. The animals were intravenous injection with TG2 (1 mg/kg, 2 mg/kg) and TPL (0.2 mg/kg). After administration for 1 h, the mice were sacrificed and the major organs (heart, liver, lung and kidney) and tumors were collected. Tissue samples were immediately weighted prior to flash freezing with dry ice before storage at -80 ℃ for future analysis. After thawing the tissues, the 1.0 g tissue was added with 2.0 mL normal saline to make homogenate. The homogenate was added methanol to precipitate protein, condensed the supernatant, then reconstituted with methanol. The contents of compounds in different organs or tumor from each group was measured by LC-MS. Three molecular weights were detected at the same time during the determination, 645.3 g/mol (TG2+Na), 483.2 g/mol (intermediate+Na), and 383.2 g/mol (TPL+Na). The LC-MS condition was used for 7.5 min running time at a flow rate of 0.3 mL/min. The eluent was monitored at 220 nm.

4.15. Statistical analysis

Statistical analysis was conducted using GraphPad Prism 8. All data were analyzed by two-way ANOVA for multiple comparisons. All experiments were performed in triplicate. The values are expressed as the mean ± SD. $P<0.05$ was considered to be statistically significant differences.

Supporting Information

The Supporting Information can be found online at

(I). Figures S1-S9,

(II). Characterization of Compounds, including NMR Spectra, HRMS Spectra and HPLC Spectra of compounds.

Author Contributions

J. Xu and Y. Zhang co-supervised the project and supplied resources. J. Xu and Y. Liu conceived the original idea, designed and planned the experiments. Y. Liu synthesized the compounds. Y. Liu, B. Liu and Y. Oyang performed cell-related research. Y. Liu, J. Huang, M. Wu, Q. Lin and J. Wu carried out the animal research. Y. Liu and J. Xu wrote the manuscript, which was edited and approved by all authors. All authors provided critical feedback and helped structure the research, analysis, and manuscript. All authors have given approval to the final version of the manuscript. These authors contributed equally.

Funding Sources

This work was funded by the National Natural Science Foundation, China (81973364), the Projects of Qihang Fund of Fujian Medical University (2017XQ2017) and Financial supports from the Centre National de la Recherche Scientifique (CNRS) and the Sorbonne Université in France.

ABBREVIATIONS

MMP, mitochondrial membrane potential

TMRE, tetramethylrhodamine ethyl ester

ROS, reactive oxygen species

MTI, mean fluorescence intensity

EGFR-TKI, epidermal growth factor-receptor-tyrosine kinase inhibitor

NSCLC, non-small cell lung cancer

Declaration of competing interest

The authors declare that they have no known competing financial interests or personal relationships that could have appeared to influence the work reported in this paper.

References

[1] S. M. Kupchan, W. A. Court, R. G. Dailey, C. J. Gilmore, R. F. Bryan, Triptolide and tripdiolide, novel antileukemic diterpenoid triepoxides from Tripterygium wilfordii, J. Am. Chem. Soc. 94 (1972) 7194-7195, https://pubs.acs.org/doi/10.1021/ja00775a078.

[2] D. Qiu, P. N. Kao, Immunosuppressive and anti-inflammatory mechanisms of triptolide, the principal active diterpenoid from the Chinese medicinal herb tripterygium wilfordii Hook. F, Drugs in R & D. 4 (2003) 1-18, https://doi.org/10.2165/00126839-200304010-00001.

[3] X. Tao, P. E. Lipsky, The Chinese anti-inflammatory and immunosuppressive herbal remedy Tripterygium wilfordii Hook F, Rheum Dis Clin North Am. 26 (2000) 29-50, https://doi.org/10.1016/S0889-857X(05)70118-6.

[4] S. J. Leuenroth, N. Bencivenga, H. Chahboune, F. Hyder, C. M. Crews, Triptolide reduces cyst formation in a neonatal to adult transition Pkd1 model of ADPKD, Nephrol. Dial. Transplant. 25 (2010) 151-153, https://doi.org/10.1093/ndt/gfp777.

[5] Q. Liu, Triptolide and its expanding multiple pharmacological functions, Int. Immunopharmacol. 11 (2011) 377-383, https://doi.org/10.1016/j.intimp.2011.01.012.

[6] H. Gao, Y. Zhang, L. Dong, X. Qu, L. Tao, Y. Zhang, J. Zhai, Y. Song, Triptolide induces autophagy and apoptosis through ERK activation in human breast cancer MCF-7 cells, Exp. Ther. Med. 15 (2018) 3413-3419, https://doi.org/10.3892/etm.2018.5830.

[7] L. Liu, G. Li, Q. Li, Z. Jin, L. Zhang, J. Zhou, X. Hu, T. Zhou, J. Chen, N. Gao, Triptolide induces apoptosis in human leukemia cells through caspase-3-mediated ROCK1 activation and MLC phosphorylation, Cell Death Dis. 4 (2013) e941-e951, https://doi.org/10.1038/cddis.2013.469.

[8] B. Giri, V. K. Gupta, B. Yaffe, S. Modi, P. Roy, V. Sethi, S. P. Lavania, S. M. Vickers, V. Dudeja, S. Banerjee, J. Watts, A. Saluja, Pre-clinical evaluation of Minnelide as a therapy for acute myeloid leukemia, J. Transl. Med. 17 (2019) 163-171, https://doi.org/10.1186/s12967-019-1901-8.

[9] R. Zhou, F. Zhang, P. He, W. Zhou, Q. Wu, J. Xu, Y. Zhou, W. Tang, X. Li, Y. Yang, Y. Li, J. Zuo, (5R)-5-hydroxytriptolide (LLDT-8), a novel triptolide analog mediates immunosuppressive effects in vitro and in vivo, Int. Immunopharmacol. 5 (2005) 1895-1903, https://doi.org/10.1016/j.intimp.2005.06.009.

[10] H. Xu, B. Liu, Triptolide-targeted delivery methods, Eur. J. Med. Chem. 164 (2019) 342-351, https://doi.org/10.1016/j.ejmech.2018.12.058.

[11] P. Zhou, X. Sun, T. Gong, Z. Zhang, L. Zhang, Conjugating glucosamine to triptolide to enhance its protective effect against renal ischemia-reperfusion injury and reduce its toxicity, J. Drug. Target. 22 (2014) 200-210, https://doi.org/10.3109/1061186X.2013.856011.

[12] Y. Fu, Q. Lin, T. Gong, X. Sun, Z. Zhang, Renal-targeting triptolide-glucosamine conjugate exhibits lower toxicity and superior

efficacy in attenuation of ischemia/reperfusion renal injury in rats, Acta Pharmacol. Sin. 37 (2016) 1467-1480, https://doi.org/10.1038/aps.2016.44.

[13] B. Qi, X. Wang, Y. Zhou, Q. Han, L. He, T. Gong, X. Sun, Y. Fu, Z. Zhang, A renal-targeted triptolide aminoglycoside (TPAG) conjugate for lowering systemic toxicities of triptolide, Fitoterapia. 103 (2015) 242-251, https://doi.org/10.1016/j.fitote.2015.04.008.

[14] N. Du, L. Song, X. Li, L. Wang, L. Wan, H. Ma, H. Zhao, Novel pH-sensitive nanoformulated docetaxel as a potential therapeutic strategy for the treatment of cholangiocarcinoma, J. Nanobiotechnology. 13 (2015) 17-27, https://doi.org/10.1186/s12951-015-0066-8.

[15] J. Zhou, C. Xi, W. Wang, X. Fu, J. Liang, Y. Qiu, J. Jin, J. Xu, Z. Huang, Triptolide-induced oxidative stress involved with Nrf2 contribute to cardiomyocyte apoptosis through mitochondrial dependent pathways, Toxicol. Lett. 230 (2014) 454-466, https://doi.org/10.1016/j.toxlet.2014.08.017.

[16] Y. Xi, W. Wang, L. Wang, J. Pan, Y. Cheng, F. Shen, Z. Huang, Triptolide induces p53-dependent cardiotoxicity through mitochondrial membrane permeabilization in cardiomyocytes-ScienceDirect, Toxicol. Appl. Pharm. 355 (2018) 269-285, https://doi.org/10.1016/j.taap.2018.07.011.

[17] Y. Xi, Y. Zhang, J. Pan, S. Chen, S. Lu, F. Shen, Z. Huang, Triptolide dysregulates glucose uptake via inhibition of IKKβ-NF-κB pathway by p53 activation in cardiomyocytes, Toxicol. Lett. 318 (2019) 1-11, https://doi.org/10.1016/j.toxlet.2019.10.001.

[18] L. Zhang, J. Chang, Y. Zhao, H. Xu, T. Wang, Q. Li, L. Xing, J. Huang, Y. Wang, Q. Liang, Fabrication of a triptolide-loaded and poly-γ-glutamic acid-based amphiphilic nanoparticle for the treatment of rheumatoid arthritis, Int. J. Nanomedicine. 13 (2018) 2051-2064, https://doi.org/10.2147/IJN.S151233.

[19] D. Hanahan, R. A. Weinberg, Hallmarks of cancer: the next generation, Cell. 144 (2011) 646-655, https://doi.org /10.1016/j.cell.2011.02.013.

[20] M. Pliszka, L. Szablewski, Glucose Transporters as a Target for Anticancer Therapy, Cancers (Basel). 13 (2021) 4184-4201, https://doi.org/10.3390/cancers13164184.

[21] M. B. Calvo, A. Figueroa, E. G. Pulido, R. G. Campelo, L. A. Aparicio, Potential role of sugar transporters in cancer and their relationship with anticancer therapy, Int J Endocrinol. 2010 (2010) 1-14, https://doi.org/10.1155/2010/205357.

[22] M. Kunkel, M. Moergel, M. Stockinger, J. Jeong, G. Fritz, H. Lehr, T. L, Whiteside, Overexpression of Glut-1 is associated with resistance to radiotherapy and adverse prognosis in squamous cell carcinoma of the oral cavity, Oral Oncol. 43 (2007) 796-803, https://doi.org/10.1016/j.oraloncology.2006.10.009.

[23] S. Ohba, H. Fujii, S. Ito, M. Fujimaki, F. Matsumoto, M. Furukawa1, J. Yokoyama, T. Kusunoki, K. Ikeda, O. Hino, Overexpression of Glut-1 in the invasion front is associated with depth of oral squamous cell carcinoma and prognosis, J. Oral. Pathol. Med. 39 (2010) 74-78, https://doi.org/10.1111/j.1600-0714.2009.00814.x.

[24] L. Szablewski, Expression of glucose transporters in cancers, Biochim Biophys Acta. 1835 (2013) 164-169, https://doi. org/10.1016/j.bbcan.2012.12.004.

[25] E. C. Calvaresi, P. J. Hergenrother, Glucose conjugation for the specific targeting and treatment of cancer, Chem Sci. 4 (2013) 2319-2333, https://doi.org/10.1002/chin.201338262.

[26] J. Fu, J. Yang, P. H. Seeberger, J. Yin, Glycoconjugates for glucose transporter-mediated cancer-specific targeting and treatment, Carbohydr Res. 498 (2020) 108195, https://doi.org/10.1016/j.carres.2020.108195.

[27] M. I. Molejon, G. Weiz, J. D. Breccia, M. I. Vaccaro, Glycoconjugation: An approach to cancer therapeutics, World J Clin Oncol. 11 (2020) 110-120, https://doi.org/ 10.5306/wjco.v11.i3.110.

[28] Q. He, I. Minn, Q. Wang, P. Xu, S. A. Head, E. Datan, B. Yu, M. G. Pomper, J. O. Liu, Targeted delivery and sustained antitumor activity of triptolide through glucose conjugation, Angew. Chem. Int. Ed. Engl. 55 (2016) 12035-12039, https://doi.org/ 10.1002/anie.201606121.

[29] E. Datan, I. Minn, P. Xu, Q. L. He, H. Ahn, B. Yu, M. G. Pomper, J. O. Liu, A Glucose-Triptolide conjugate selectively targets cancer cells under hypoxia, iScience. 23 (2020) 101536-101616, https://doi.org/10.1016/j.isci.2020.101536.

[30] M. Patra, S. G. Awuah, S. J. Lippard, Chemical approach to positional isomers of glucose-platinum conjugates reveals specific cancer targeting through glucose-transporter mediated uptake in vitro and in vivo, J. Am. Chem. Soc. 138 (2016) 12541-12551, https: //doi.org/10.1021/jacs.6b06937.

[31] K. Kapoor, J. S. Finer-Moore, B. P. Pedersen, L. Caboni, A. Waight, R. C. Hillig, P. Bringmann, I. Heisler, T. Müllere, H. Siebeneicher, and R. M. Stroud, Mechanism of inhibition of human glucose transporter GLUT1 is conserved between cytochalasin B and phenylalanine amides, Proc Natl Acad Sci U S A. 113 (2016) 4711-4716, https://doi.org/10.1073/pnas.1603735113.

[32] F. Zhang, A. Vasella, Regioselective synthesis of 1I, 1II, 5I, 5II, 6I, 6I, 6II, 6II-2H8-cellobiose, Carbohydr. Res. 342 (2007) 2546-2556, https://doi.org/10.1016/j.carres.2007.07.017.

[33] P. Noel, S. Hussein, S. Ng, C. E. Antal, W. Lin, E. Rodela, P. Delgado, S. Naveed, M. Downes, Y. Lin, R. M. Evans, D. D. V. Hoff, H. Han, Triptolide targets super-enhancer networks in pancreatic cancer cells and cancer-associated fibroblasts, Oncogenesis. 9 (2020) 100-111, https://doi.org/10.1038/s41389-020-00285-9.

[34] J. Pan, RNA polymerase – An important molecular target of triptolide in cancer cells, Cancer Lett. 292 (2010) 149-152, https:// doi.org/10.1016/j.canlet.2009.11.018.

[35] O. Tamgue, M. Lei, Triptolide Promotes Senescence of Prostate Cancer Cells Through Histone Methylation and Heterochromatin Formation, Asian. Pac. J. Cancer. Prev. 18 (2017) 2519-2526, https://doi.org/10.22034/APJCP.2017.18.9.2519.

[36] C. Dienemann, B. Schwalb, S. Schilbach, P. Cramer, Promoter distortion and opening in the RNA Polymerase II cleft, Mol. Cell. 73 (2018) 97-106, https://doi.org/10.1016/j.molcel.2018.10.014.

[37] B. J. Greber, T. H. D. Nguyen, J. Fang, P. V. Afonine, P. D. Adams, E. Nogales, The cryoelectron microscopy structure of human transcription factor IIH, Nature. 549 (2017) 414-417, https://doi.org/10.1038/nature23903.

[38] S. Vispe, L. Devries, L. Creancier, J. Besse, S. Breand, D. J. Hobson, J. Q. Svejstrup，J. Annereau, D. Cussac, C. Dumontet, N. Guilbaud, J. Barret, C. Bailly, Triptolide is an inhibitor of RNA polymerase I and II–dependent transcription leading predominantly to down-regulation of short-lived mRNA, Mol. Cancer. Ther. 8 (2009) 2780-2790.

[39] B. Chance, H. Sies, A. Boveris, Hydroperoxide metabolism in mammalian organs, Physiol Res. 59 (1979) 527-605, https://doi.org/ 10.1152/physrev.1979.59.3.527.

[40] G. J. Gores, C. E. Flarsheim, T. L. Dawson, A. Nieminen, B. Herman, J. J. Lemasters, Swelling, reductive stress, and cell death during chemical hypoxia in hepatocytes, Am. J. Physiol. 257 (1989) C347-C354, https://doi.org/10.1152/ajpcell.1989.257.2.C347.

[41] T. L. Dawson, G. J. Gores, A. Nieminen, B. Herman, J. J. Lemasters, Mitochondria as a source of reactive oxygen species during reductive stress in rat hepatocytes, Am. J. Physiol. 264 (1993) C961-C967, https://doi.org/10.1152/ajpcell.1993.264.4.C961.

[42] J. Kim, T. Qian, J. J. Lemasters, Mitochondrial permeability transition in the switch from necrotic to apoptotic cell death in ischemic rat hepatocytes, Gastroenterol. 124 (2003) 494-503, https://doi.org/10.1053/gast.2003.50059.

[43] F. Bray, J. Ferlay, I. Soerjomataram, R. L. Siegel, L. A. Torre, A. Jemal, Global cancer statistics 2018: GLOBOCAN estimates of incidence and mortality worldwide for 36 cancers in 185 countries, Ca. Cancer. J. Clin. 68 (2018) 394-424, https://doi.org/10.3322 /caac.21660.

[44] A. Tartarone, R. Lerose, Clinical approaches to treat patients with non-small cell lung cancer and epidermal growth factor receptor tyrosine kinase inhibitor acquired resistance, Ther. Adv. Respir. Dis. 9 (2015) 242-250, https://doi.org/10.1177/1753465815587820.

[45] W. Pao, J. Chmielecki, Rational, biologically based treatment of EGFR-mutant non-small-cell lung cancer, Nat. Rev. Cancer. 10 (2010) 760-774, https://doi.org/10.1038/nrc2947.

[46] L. Xu, Y. Qiu, H. Xu, W. Ao, W. Lam, X. Yang, Acute and subacute toxicity studies on triptolide and triptolide-loaded polymeric micelles following intravenous administration in rodents, Food Chem Toxicol. 57 (2013) 371-379, https://doi.org/10.1016/j.fct.2013.03.044.

[47] J. C. Degenstein, P. Murria, M. Easton, H. Sheng, M. Hurt, A. R. Dow, J. Gao, J. J. Nash, R. Agrawal, W. N. Delgass, F. H. Ribeiro, H. I. Kenttamaa, Fast pyrolysis of 13C-labeled cellobioses: gaining insights into the mechanisms of fast pyrolysis of carbohydrates, J. Org. Chem. 80 (2015) 1909-1914, https://doi.org/10.1021/jo5025255.

[48] W. Lu, L. Navidpour, S. D. Taylor, An expedient synthesis of benzyl 2,3,4-tri-O-benzyl-beta-D-glucopyranoside and benzyl 2,3,4-tri-O-benzyl-beta-D-mannopyranoside, Carbohydr. Polym. 340 (2005) 1213-1217, https://doi.org/10.1016/j.carres.2005.02.013.

Graphical abstract

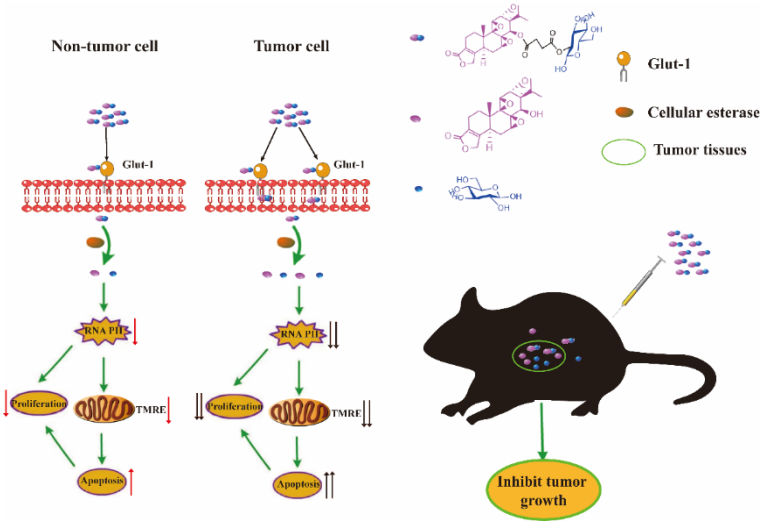

TG2 conjugated by triptolide and D-glucose C2-OH has a stronger selective antitumor activity than triptolide due to selective transport of TG2 into tumor cells via glucose transporters.